Environment Canada Environnement Canada

III

National Hydrology Research Institute

and 27

SEE PAGES 22-25 FOR STREAMFLOW MEASUREMENT DISCUSSION

NHRI PAPER NO. 40
IWD SCIENTIFIC SERIES NO. 162

Observations on Ice Cover and Streamflow in the Yukon River near Whitehorse during 1985/86

M.E. Alford and E.C. Carmack

NHRI

INLAND WATERS/LANDS DIRECTORATE
NATIONAL HYDROLOGY RESEARCH INSTITUTE
NATIONAL HYDROLOGY RESEARCH CENTRE
SASKATOON, SASKATCHEWAN, 1987
(Disponible en français sur demande)

Environment Canada Environnement Canada

National Hydrology Research Institute

NHRI PAPER NO. 40
IWD SCIENTIFIC SERIES NO. 162

Observations on Ice Cover and Streamflow in the Yukon River near Whitehorse during 1985/86

M.E. Alford* and E.C. Carmack†

*Formerly with:
Water Survey of Canada
Water Resources Branch
Inland Waters Directorate
Pacific and Yukon Region
Whitehorse, Yukon Territory

Current address:
Yukon Expeditions
127 Alsek
Whitehorse, Yukon Territory

†Inland Waters Directorate
National Hydrology Research Institute
National Hydrology Research Centre
Saskatoon, Saskatchewan

Current address:
Fisheries and Oceans Canada
Institute of Ocean Sciences
9860 West Saanich Road
Sidney, British Columbia

NHRI

INLAND WATERS/LANDS DIRECTORATE
NATIONAL HYDROLOGY RESEARCH INSTITUTE
NATIONAL HYDROLOGY RESEARCH CENTRE
SASKATOON, SASKATCHEWAN, 1987

(Disponible en français sur demande)

Published by authority of
the Minister of the Environment

Contents

Tables

Illustrations

Abstract

The Yukon Ice Seasonality Experiment (YISEX) was initiated to obtain a better understanding of physical processes affecting the ice cover on northern lake and river systems. Subsequently, studies on the winter hydraulics and ice regime along a 4.3-km reach of the Yukon River at Whitehorse were carried out during the winters of 1983/84 and 1984/85. This report on the third year (1985/86) of the YISEX study documents meteorological, hydrological, and ice conditions, investigates the effects of specific ice conditions (e.g., leads, ice fronts, frazil deposits, and ice ripples) on river hydraulics, and introduces a new method for the measurement of river discharge in winter. A summary comparison of the three winters is presented.

The winter of 1985/86 was relatively mild, but marked by short-duration extremes in both temperature and snowfall. At freeze-up, air temperatures were below normal while snowfall was two to three times above normal; in midwinter, air temperatures were above normal and snowfall was below normal; at breakup, air temperatures were below normal. Because of these weather conditions, freeze-up was initiated earlier than normal, but took longer to complete. Breakup was later than normal. Also, the rate of ice front advance through the reach, the main process of freeze-up, was highly irregular.

Frazil dam formation followed the same spatial pattern as observed in earlier years, occupying about 30% to 40% of the cross-sectional area of the river. Deposition at a given site is influenced by velocity patterns, stream geometry, and the underside roughness of the ice cover. In general, frazil dams appear to reach maximum size immediately after freeze-up, and then to erode gradually toward spring.

In relation to the hydraulic resistance of the reach, water levels at all stations increased rapidly at freeze-up, declined gradually during midwinter, and fell sharply after breakup. Ice front advance was found to be the main process affecting water level at any given location. Significant variations in surface slope within the reach associated with overflow were observed during periods of mild weather.

Two new aspects of ice ripples (wavelike features at the ice/water interface) were noted. First, ripples may form at any time in winter wherever water temperatures rise above the freezing point, such as near the outlets of lakes and reservoirs. Second, ripples migrate through white (overflow) ice much faster than through black (thermal) ice, and thus rapidly reduce the strength of the ice cover during breakup.

An examination of velocity profiles confirmed earlier observations by Alford and Carmack that a point of minimum variance in plots of normalized velocity versus normalized depth existed at the 0.4 depth, which is also the depth of V_{max}. It was found that the application of a coefficient of 0.86 to velocities observed at the 0.4 depth yielded a value close to the mean velocity of the full profile. Using this information, a new method for computing streamflows in ice-covered rivers (called the "486" method) is proposed.

Résumé

L'Expérience de saisonnalité glacielle du Yukon (ESAGY) a été mise sur pied en vue d'améliorer les connaissances sur les processus physiques qui influent sur la couverture de glace dans les réseaux hydrographiques (lacs et cours d'eau) du Nord. Durant les hivers de 1983-1984 et de 1984-1985, on a étudié les conditions hydrauliques et le régime des glaces dans un tronçon de 4.3 km du fleuve Yukon à Whitehorse. Le présent rapport porte sur la troisième année (1985-1986) de l'étude. On y présente des données sur les conditions météorologiques et hydrologiques ainsi que sur les conditions des glaces; on y étudie les effets de conditions particulières (par exemple, chenaux, fronts de glace, dépôts de frasil et rides) sur les caractéristiques hydrauliques du fleuve, et on y introduit une nouvelle méthode de mesure du débit en hiver. Un résumé comparatif des conditions observées au cours des trois hivers d'étude est présenté.

L'hiver de 1985-1986 a été relativement doux, mais on a enregistré des extrêmes de courte durée en ce qui concerne la température et l'enneigement. Au moment de la prise de la glace, les températures de l'air étaient inférieures à la normale, tandis que l'enneigement était de deux à trois fois supérieur à la normale. Au milieu de l'hiver, les températures de l'air étaient au-dessus de la normale, tandis que l'enneigement était inférieur à la normale; au moment de la débâcle, les températures de l'air étaient inférieures à la normale. Ces conditions météorologiques se sont traduites par une prise des glaces plus tôt que la normale, mais plus lente, par une débâcle plus tard que la normale et aussi par une progression très irrégulière du front de glace (principal processus de prise des glaces) dans le tronçon.

On a observé les mêmes caractéristiques spatiales pour la formation de la barrière de frasil que par les années passées, cette barrière occupant de 30 % à 40 % environ de la superficie de la section transversale du fleuve. Le dépôt à un endroit donné dépend de la vitesse d'écoulement, de la géométrie du cours d'eau et de la rugosité de la surface inférieure de la couverture de glace. En général, les barrières de frasil semblent atteindre leur dimension maximale immédiatement après la prise de la glace puis elles s'érodent graduellement vers le printemps.

En ce qui concerne la résistance hydraulique, le niveau de l'eau a augmenté rapidement à toutes les stations au moment de la prise des glaces, il a diminué graduellement au milieu de l'hiver puis il a baissé de façon marquée après la débâcle. La progression du front de glace est le principal processus qui influe sur le niveau de l'eau à un endroit donné. Des variations significatives de la pente de la ligne d'eau dans le tronçon, lesquelles étaient associées à des débordements, ont été observées au cours des périodes de temps doux.

Deux nouvelles caractéristiques des rides de glace (ondulations à l'interface glace-eau) ont été observées. Premièrement, ces rides peuvent se former n'importe quand au cours de l'hiver partout où les températures de l'eau augmentent au-dessus du point de congélation, par exemple près des exutoires des lacs et des réservoirs. Deuxièmement, les rides se propagent dans la glace blanche (de débordement) beaucoup plus rapidement que dans la glace noire (thermique) et, par conséquent, elles réduisent rapidement la résistance de la couverture de glace au moment de la débâcle.

Un examen des profils des vitesses d'écoulement a permis de confirmer des observations d'Alford et Carmack que dans les graphiques de la vitesse normalisée en fonction de la profondeur normalisée, la variance est minimale à une profondeur égale aux 4/10 de la profondeur totale, ce qui est également la profondeur où l'on trouve V_{max}. On a constaté que l'application d'un coefficient de 0.86 aux vitesses observées aux 4/10 de la profondeur donnait une valeur près de la vitesse moyenne pour tout le profil. À partir de cette constatation, on propose une nouvelle méthode (appelée méthode 486) pour le calcul de l'écoulement dans les cours d'eau recouverts de glace.

Observations on Ice Cover and Streamflow in the Yukon River near Whitehorse during 1985/86

M.E. Alford and E.C. Carmack

INTRODUCTION

The goal of the Yukon Ice Seasonality Experiment (YISEX) is to acquire a better understanding of processes affecting the seasonal ice cover of the rivers and lakes of northern Canada. To this end, an ice hydraulics study was initiated along a 4.3-km reach of the Yukon River near Whitehorse during the winter of 1983/84 and continued in 1984/85 (Alford and Carmack, 1987a, 1987b). This report relates to observations made during the third winter of study (1985/86) and the effect of a different sequence of weather patterns on the formation of the ice cover.

This report has three objectives. The first is to document the meteorological, hydrological, and ice conditions, especially with regard to patterns of freeze-up and breakup. The second is to focus on processes that appear to have an important effect on the hydraulic characteristics of the river, including lead closure through edge ice growth, ice front advance, frazil deposition, and ice ripple formation. The third is to introduce and test the idea that single-point observations of velocity can yield, with an appropriate coefficient, estimates of vertically averaged velocity that satisfy the standards of accuracy set by the Water Survey of Canada. Coincident with the above, additional velocity profiles were obtained to support observations from 1983/84 and 1984/85, which identified a point of minimum variance in the vertical velocity profile.

Study Area

The reach of the Yukon River near Whitehorse extending from the Robert Campbell Bridge to the narrows 4.3 km downstream was studied (Fig. 1). Here, the river drains an area of 19 400 km^2 and has a mean annual streamflow of 240 $m^3 s^{-1}$.

Within this reach, the flow has been modified by the construction of two upstream dams. The first, located below the outlet of Marsh Lake, provides upstream storage. The second, located at Whitehorse Rapids, is the Northern Canada Power Commission's (NCPC) hydroelectric power station. At present, the discharge at Whitehorse reflects the combined regulation of the two dams, subject to both structural and legal limitations. Specifically, the water level behind the dam in Schwatka Lake cannot rise above 653.34 m or fall below 652.27 m. Regulation of discharge is especially critical during freeze-up, as this is the time when the reach at Whitehorse exhibits maximum resistance to flow, and is thus sensitive to flooding.

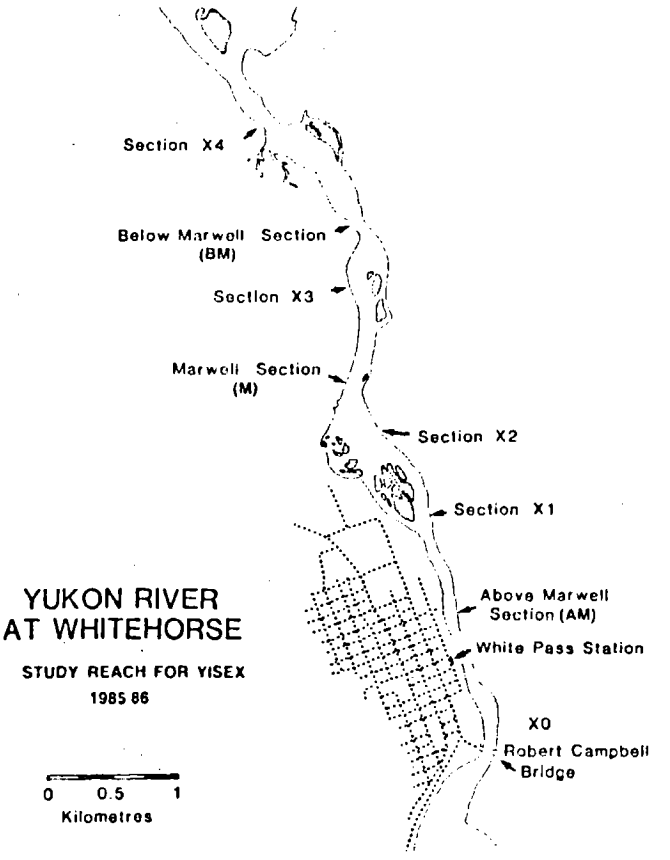

Figure 1. Study area and station locations.

Measurements

Water levels were recorded daily at five stations, X0, AM, M, BM, and X4, during freeze-up, and at the first four locations for the duration of the winter. The latter four stations were the same as those used in the previous studies.

The X0 station was added for the 1985/86 study to extend the coverage of river gradient closer to the point of maximum ice front advance. To minimize aliasing problems associated with any diurnal variations in water level, an attempt was made to take readings at approximately the same time each day.

At each of the principal cross-sections noted above, measurements were obtained of ice thickness, frazil accumulation, cross-sectional area, and flow velocity at various times throughout the winter. Measurement techniques were the same as those described in Alford and Carmack (1987a). However, a lighter, more compact metering sled, heated by two Coleman (Model 519) radiant heaters, was designed and used throughout the season with considerable success.

Daily values of streamflow were obtained from the total amount of water passing the NCPC dam at Whitehorse Rapids. Air temperature and barometric pressure were recorded at 07:00 h at the Alford residence in Riverdale approximately 1 km from the study reach and approximately 10 m above water level. Although not reported here, meteorological data were recorded by the Atmospheric Environment Service at Whitehorse Airport, which is approximately 1 km from the study reach and approximately 60 m above water level.

Photographs were taken of structural features of ice whenever such were deemed necessary. To observe changes that took place on the underside of the ice during spring, several blocks were extracted from the cover, inverted, and photographed. In addition, underwater video photos were taken of the frazil dams to investigate textural features of this horizon and to examine current meter behaviour at the slush/water interface.

OBSERVATIONS AND COMPARISONS

Meteorology and Hydrology

Figures 2 and 3 show air temperature and barometric pressure as functions of time; Table 1 summarizes the mean monthly meteorological conditions. Comparison with earlier data (see Alford and Carmack, 1987a, 1987b) shows that the winter of 1985/86 was notably warmer than that of the previous two years. The winter began with episodes of cold (-20°C) weather in November, but then warmed, especially in December and early January. The unseasonably warm temperatures in early January resulted in considerable flooding (overflow) of the ice covering the reach. The winter of 1985/86 also displayed very few periods of extreme cold. Only in late November and late February did temperatures reach -30°C.

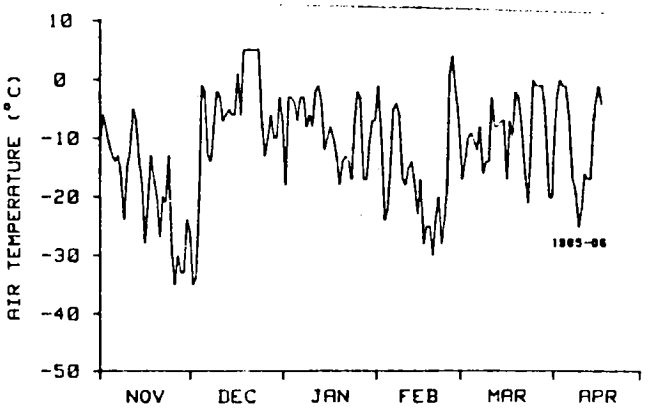

Figure 2. Air temperature as a function of time.

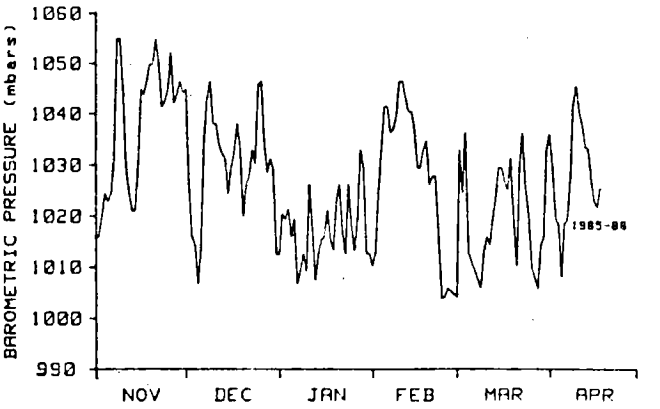

Figure 3. Barometric pressure as a function of time.

Table 1. Mean Monthly Meteorological Conditions for the Three Study Years

Month	1983/84	1984/85	1985/86
	Mean monthly air temperature		
Nov.	-9.3	-10.5	-18.2
Dec.	-23.9	-18.2	-6.7
Jan.	-12.8	-4.7	-7.8
Feb.	-6.3	-18.2	-12.8
Mar.	0.1	-6.1	-7.3
Apr.	2.6	-1.0	-4.5
Mean	-8.3	-9.8	-9.6
	Degree days below 0°C per month		
Nov.	-279	-315	-546
Dec.	-741	-564	-208
Jan.	-397	-146	-242
Feb.	-183	-510	-358
Mar.	3	-189	-226
Apr.	78	-30	-135
	Snowfall per month (cm)		
Nov.	5.0	19.8	24.0
Dec.	9.2	43.0	11.2
Jan.	32.4	43.2	24.8
Feb.	15.8	33.4	5.4
Mar.	8.6	12.2	62.2
Apr.	1.4	15.6	28.6
Total	72.4	167.2	156.2

A second major difference in weather conditions was the very high snowfall experienced in March 1986, which was three times the average and the highest recorded for that month in 30 years.

Figure 4 shows streamflow as a function of time. The flow in 1985/86 was both lower (by 10% to 20%) and less variable than in the previous two years. Since flow can be controlled within narrow limits by the dam at Whitehorse Rapids, any adjustments made for the purpose of turbine switching, maintenance, or calibration can result in short-term fluctuations in streamflow. During 1985/86, a newly installed turbine (the fourth wheel) was used almost exclusively, resulting in a more stable streamflow.

Figure 4. Streamflow as a function of time.

Ice Cover Distributions

The freezing sequence observed in 1985/86 is summarized in Figures 5 and 6 (see also Appendix). Edge ice began forming in the back channels of the river on November 1. A visual reconnaissance of the Yukon River between upper Lake Laberge and Whitehorse on November 7 revealed that the ice front had progressed to a point 1.3 km downstream from the mouth of the Takhini River, or about 14 km below the study reach. At this time, a 1.7-km long ice bridge crossed the river at the mouth of the Takhini, and large (30- to 50-m diameter) ice pans were observed running in the river. By November 9 the ice front had progressed to X4.

Freeze-up of the study reach in 1985 was similar to previous years (cf. Alford and Carmack, 1987a, 1987b), characterized by a combination of edge ice closing inwards to form a narrow channel along the velocity core, and the progressive upstream advance of the ice front by the deposition at its leading edge of frazil ice, pans, and floes. Then, between November 9 and December 9, coincident with cold weather, thin (3-mm thick) platelets were observed in the remaining open water; hence the ice front

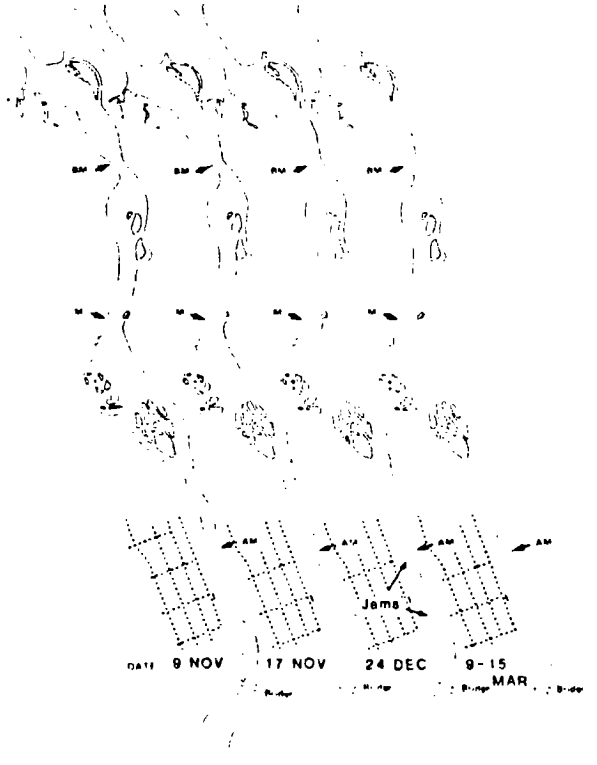

Figure 5. Maps of ice cover during freeze-up.

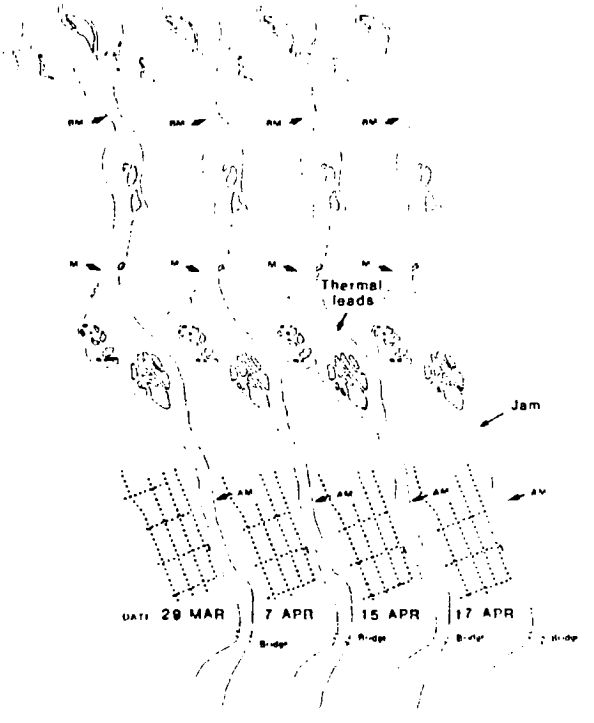

Figure 6. Maps of ice cover during midwinter and breakup.

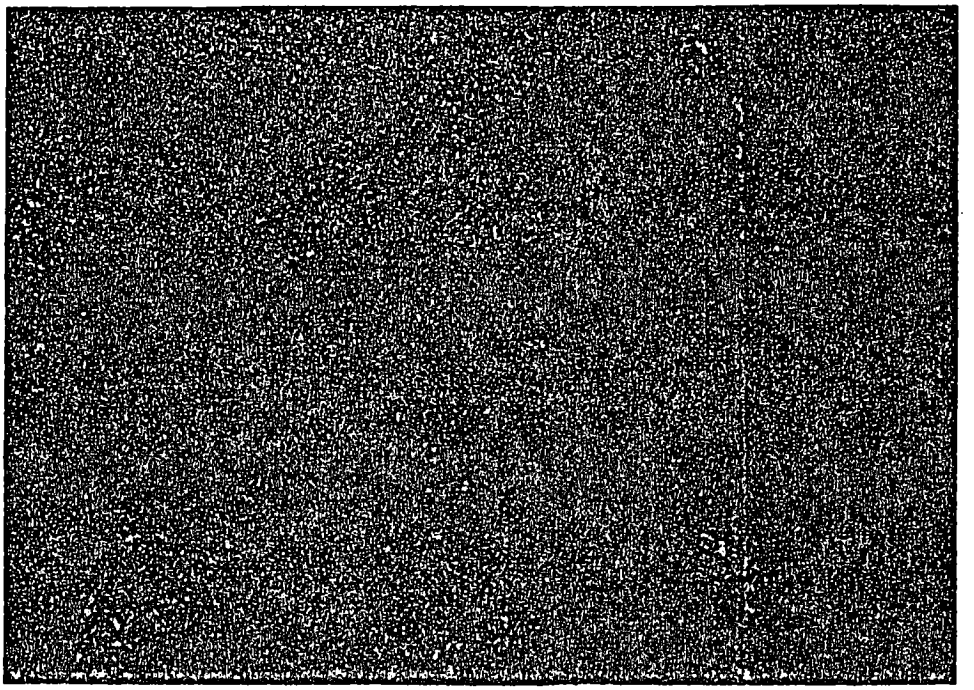

Figure 7. Surface texture of the ice front observed between BM and M (November 16, 1985).

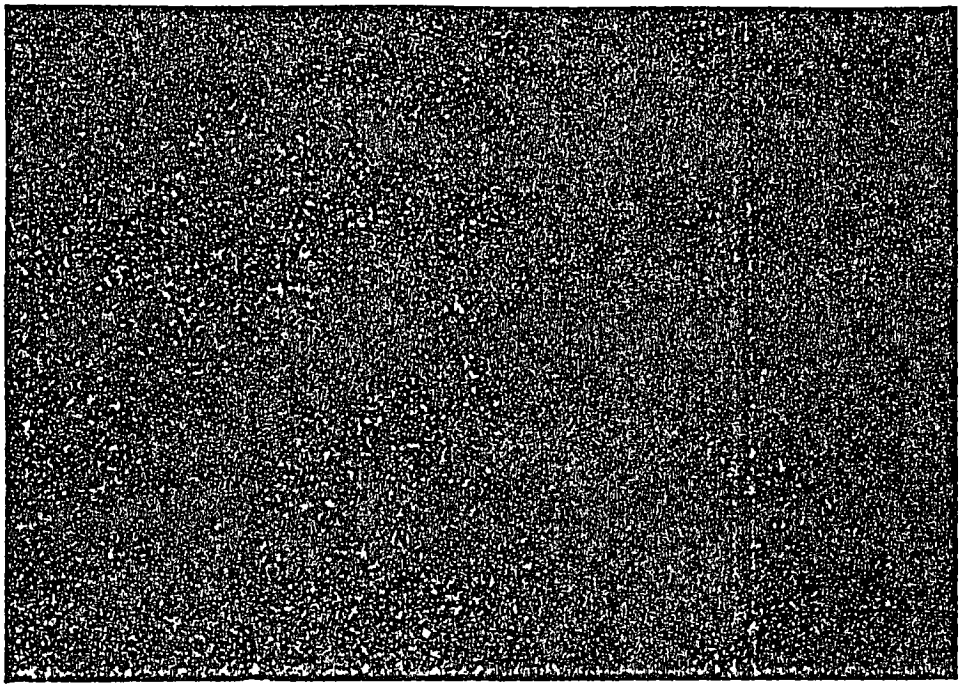

Figure 8. Close-up view of platelets making up the ice front (November 16, 1985).

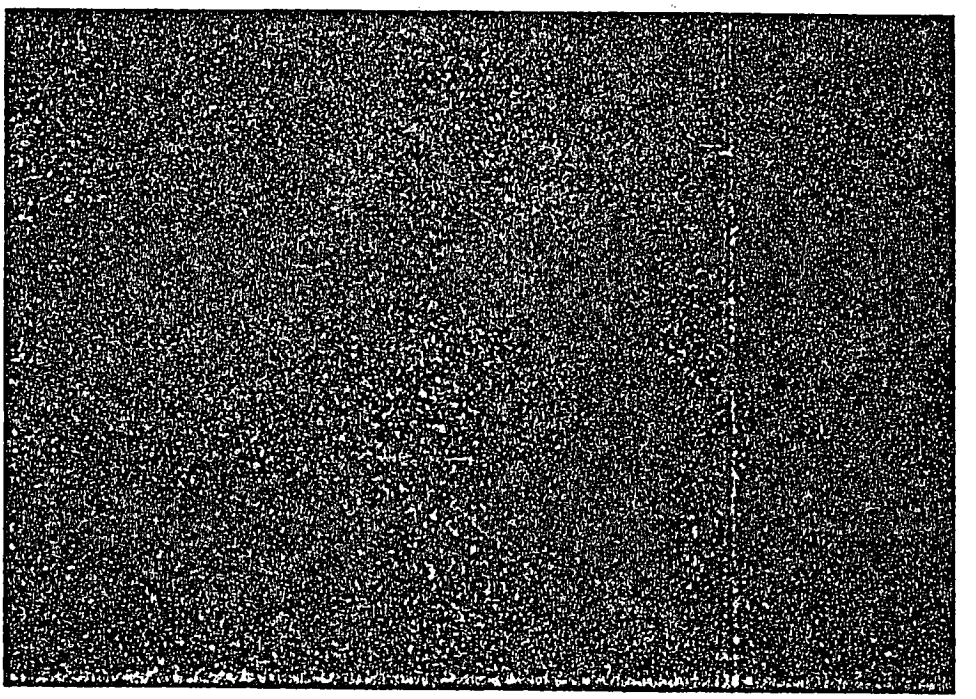

Figure 9. Heated metering sled on the river near M following an overflow event and subsequent re-freezing of the flooded ice and snow cover (December 23, 1985).

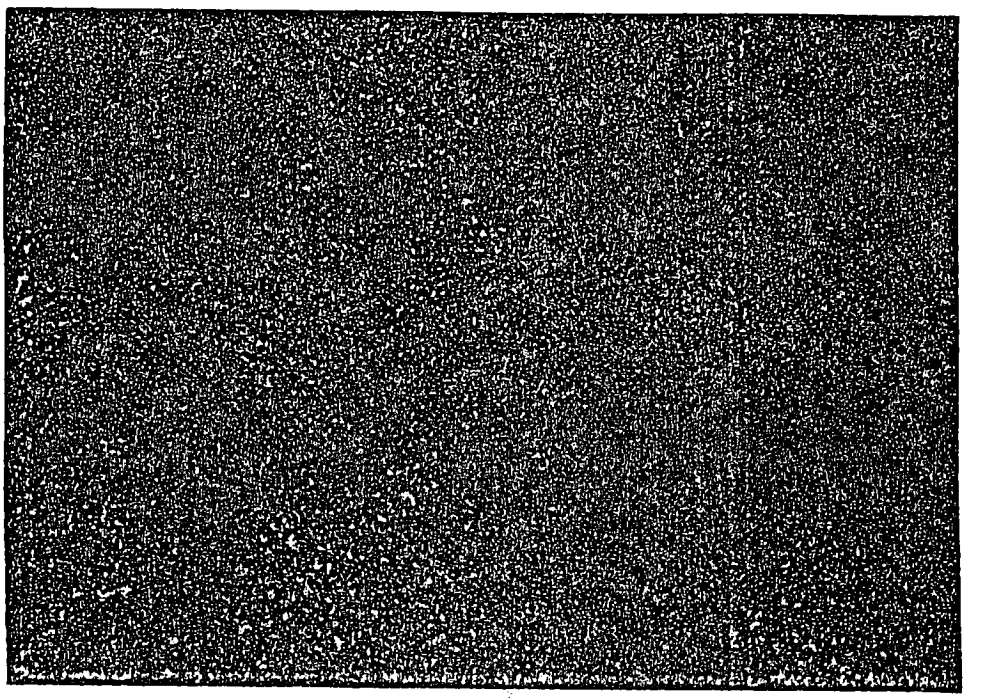

Figure 10. Ripples observed on the underside of ice at the ice jam above the Robert Campbell Bridge during freeze-up (December 21, 1985).

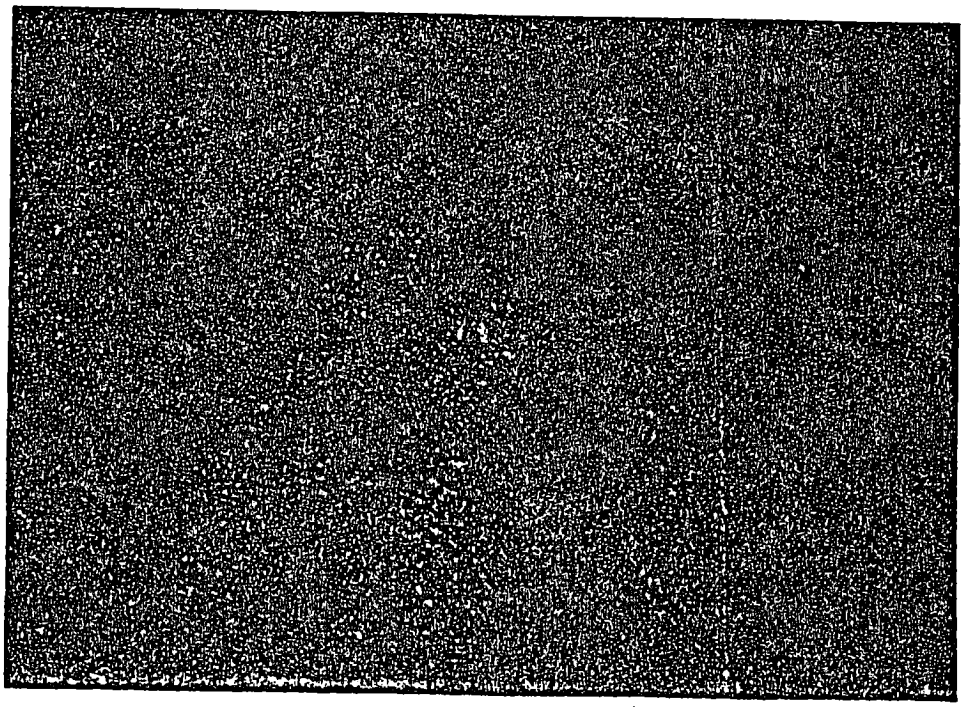

Figure 11. Large pan about to lodge at the ice front immediately above X0 (February 11, 1986).

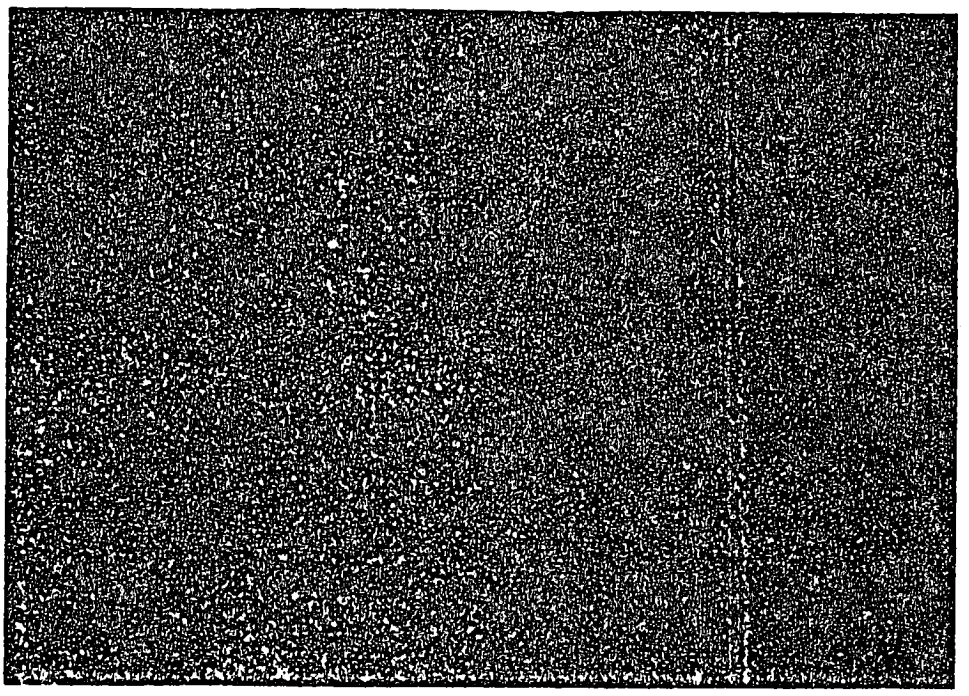

Figure 12. Subsequent lodging of pans upstream from the large pan shown in Figure 11, and the attendant areas of open water (February 16, 1986).

advanced from X4 to a point 150 m below AM as the result of a steady agglomeration of these platelets (Fig. 7). Inspection of these plates revealed that they were, in turn, a collage-like structure made up of yet thinner platelets, presenting a scaly appearance (Fig. 8). These plates would upend on contact with the ice front and freeze in that position to yield a very rough ice surface.

Through the remainder of December and the first half of January, coincident with unseasonably warm weather, a generally smoother ice cover developed between M and AM from the juxiposition of large pans that had once been edge ice along the reach upstream from X0.

Because of especially warm weather in mid-December and in the second and last weeks of February, the ice cover was prone to flooding. This flooding was related to the increased streamflows and water levels associated with warm air temperatures, and to the presence of large pans broken away from edge ice upstream. At times, these pans would upend at the ice front and divert the flow up and over the existing cover, causing overflow. During such times, the overflowing water reached depths of up to 0.15 m, saturating the snow cover and making travel over the ice difficult. The subsequent freezing of the surface water and flooded snow resulted in additional layers (approximately 0.40 m) of so-called white ice forming above the thermal or black ice cover (Fig. 9).

A surprising observation was the occurrence of ice ripples during freeze-up. These were found serendipitously on an overturned pan of edge ice in the reach between the Whitehorse Rapids dam and the Robert Campbell Bridge (Fig. 10). While such features are ubiquitous at breakup, their formation during freeze-up was unexpected; their possible origin is discussed later.

The process of ice front advance by the lodging of large pans derived from edge ice upstream continued through much of the winter (Fig. 11). Because of the irregular shape of such pans, the resulting cover had many large holes in it (Fig. 12).

The maximum upstream advance of the continuous cover was 50 m downstream from the Robert Campbell Bridge from March 9 to 15. However, pans wedging against the single pier of the bridge resulted in an isolated cover which, at maximum extension, reached a point 350 m upstream.

The first signs of breakup in late March and early April included the occurrence of overflow at both ice fronts and along the edges of the cover. By April 9 thermal leads occupied the reach upstream from M. However, record-breaking low temperatures between April 8 and 15 slowed the process of breakup, so that it was not until April 22 that the reach was open. At this time, only edge and grounded ice remained along the reach.

Daily values of areal ice coverage were computed from the maps shown in the Appendix. These data (Fig. 13, Table 2) reveal a period of rapid increase in mid-November, followed by a far slower increase in coverage later on. Because of the unseasonably low temperatures during the first half of April, the plot of ice cover as a function of time is stepped.

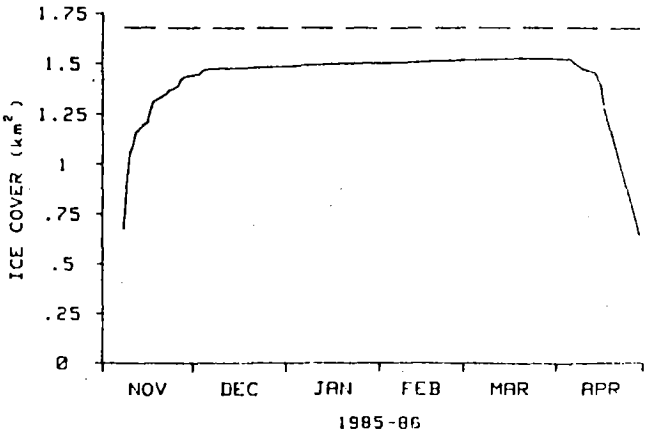

Figure 13. Surface area of ice cover from X4 to the generating station as a function of time.

Figure 14 shows the mean ice thickness at M as a function of time; Figure 15 shows the estimated volume of ice within the reach, obtained as the product of areal ice coverage times mean ice thickness at M. Both curves follow a similar trend of moderate increase during freeze-up, steady conditions in midwinter, and rapid but intermittent decreases at breakup.

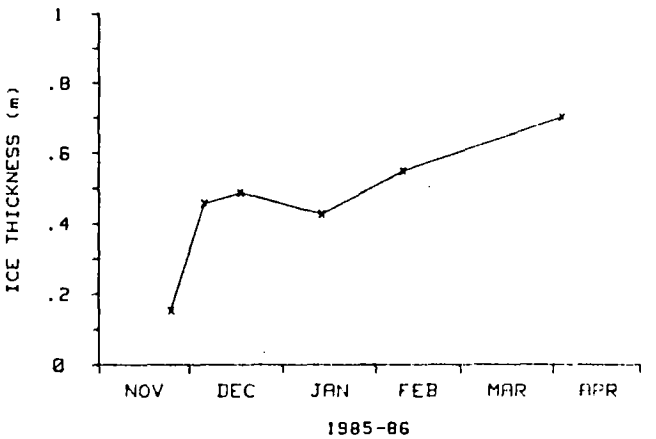

Figure 14. Mean ice thickness at M as a function of time.

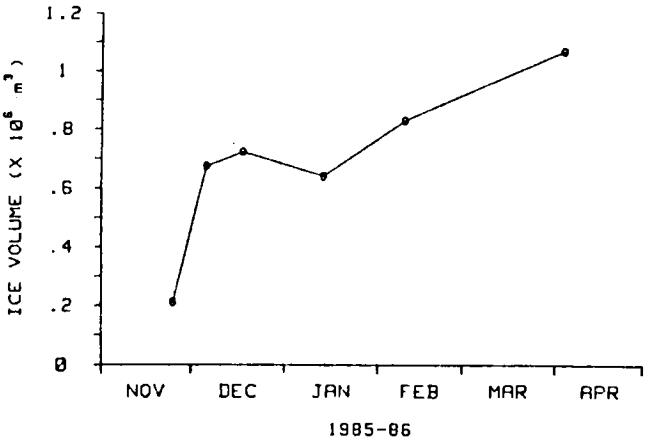

Figure 15. Estimated ice volume in the reach as a function of time.

Table 2. Area of Ice Cover and Volume of Ice during the Winter of 1985/86

Date	AM to M Open (km^2)	AM to M Covered (km^2)	AM to M Coverage (%)	NCPC dam to X4 Open (km^2)	NCPC dam to X4 Covered (km^2)	NCPC dam to X4 Coverage (%)
85-11-08	0.26	0.19	43	0.91	0.60	40
85-11-09	0.24	0.21	48	0.72	0.79	53
85-11-10	0.23	0.22	49	0.57	0.94	63
85-11-11		0.22	50		0.98	65
85-11-12		0.24	55		1.04	69
85-11-15		0.24	55		1.08	71
85-11-16		0.24	55		1.08	72
85-11-17		0.25	56		1.14	76
85-11-18		0.28	63		1.18	78
85-11-20		0.31	69		1.19	79
85-11-21		0.31	70		1.20	80
85-11-22		0.32	71		1.21	80
85-11-23		0.34	76		1.23	81
85-11-25		0.36	79		1.24	82
85-11-26		0.36	81		1.24	83
85-11-27		0.37	83		1.27	85
85-11-28		0.37	84		1.29	85
85-11-29		0.38	85		1.29	86
85-12-01		0.38	85		1.29	86
85-12-03		0.38	86		1.30	86
85-12-04		0.40	90		1.31	87
85-12-05		0.43	95		1.32	88
85-12-06		0.43	95		1.32	88
85-12-07		0.43	95		1.32	88
85-12-08		0.43	97		1.32	88
85-12-10		0.43	97		1.32	88
85-12-14		0.44	98		1.32	88
85-12-19		0.44	99		1.33	88
85-12-20		0.44	99		1.33	88
85-12-21		0.44	99		1.33	88

Table 2. Continued

Date	AM to M Open (km^2)	AM to M Covered (km^2)	AM to M Coverage (%)	NCPC dam to X4 Open (km^2)	NCPC dam to X4 Covered (km^2)	NCPC dam to X4 Coverage (%)
85-12-23		0.44	99		1.33	88
85-12-24		0.44	99		1.33	88
85-12-26		0.45	100		1.33	88
86-01-03		0.45	100		1.33	89
86-01-05		0.45	100		1.34	89
86-01-07		0.45	100		1.34	89
86-01-08		0.45	100		1.34	89
86-01-14		0.45	100		1.34	89
86-01-15		0.45	100		1.34	89
86-01-19		0.45	100		1.35	90
86-01-20		0.45	100		1.35	90
86-01-21		0.45	100		1.35	90
86-01-22		0.45	100		1.35	90
86-01-23		0.45	100		1.35	90
86-01-25		0.45	100		1.35	90
86-01-26		0.45	100		1.35	90
86-01-27		0.45	100		1.35	90
86-01-30		0.45	100		1.35	90
86-01-31		0.45	100		1.35	90
86-02-02		0.45	100		1.35	90
86-02-04		0.45	100		1.35	90
86-02-06		0.45	100		1.35	90
86-02-09		0.45	100		1.35	90
86-02-10		0.45	100		1.35	90
86-02-11		0.45	100		1.35	90
86-02-13		0.45	100		1.35	90
86-02-14		0.45	100		1.35	90
86-02-18		0.45	100		1.36	90
86-02-20		0.45	100		1.36	90
86-02-22		0.45	100		1.36	90
86-02-23		0.45	100		1.36	90
86-02-24		0.45	100		1.36	90
86-02-27		0.45	100		1.36	90
86-03-01		0.45	100		1.36	90
86-03-08		0.45	100		1.36	91
86-03-15		0.45	100		1.37	91
86-03-25		0.45	100		1.37	91
86-03-27		0.45	100		1.37	91
86-03-28		0.45	100		1.37	91
86-03-29		0.45	100		1.37	91
86-03-30		0.45	100		1.37	91
86-04-04		0.45	100		1.37	91
86-04-05		0.45	100		1.36	91
86-04-06		0.45	100		1.36	90
86-04-07		0.43	96		1.35	90
86-04-10		0.41	92		1.32	88
86-04-14		0.41	91		1.31	87
86-04-15		0.39	86		1.27	85
86-04-16		0.34	77		1.25	83
86-04-17		0.32	71		1.15	76
86-04-29		0.28	62		0.58	38

A comparison of the dates of freeze-up and breakup and the duration of continuous cover at each of the primary sections for each of the three study years is given in Table 3. In general, the early date of freeze-up in 1985/86, combined with the mild temperatures that led to overflow and the formation of white ice, resulted in an ice cover that was about 0.25 m thinner than that of 1984/85, but similar to that of 1983/84. Even though 1985/86 was the warmest of the three winters, it had the longest duration of ice cover. This shows that the meteorological conditions that prevail at the critical times of freeze-up and breakup are the ones that govern the duration of ice cover.

Frazil Dam Characteristics

Frazil dams are defined as accumulations of frazil ice particles (slush) on the undersides of ice covers. The frazil itself is presumed to form in turbulent, open water areas upstream from the stable ice cover during periods of intense cooling (Osterkamp, 1978; Martin, 1981; Tsang, 1982; Osterkamp and Gosink, 1983). Whether or not frazil adheres at a given location depends upon flow velocity, ice cover roughness, and the frazil's inherent state of "stickiness."

The frazil dam at Marwell has been described in earlier reports (Alford and Carmack, 1987a, 1987b), where we noted that the dam appeared to form every year and that the basic shape of the dam was constant from year to year. We also observed that the cross-sectional area of the dam appeared to reach a maximum immediately after freeze-up and to decrease thereafter, slowly in midwinter and rapidly just prior to breakup.

Figures 16 and 17 show changes in the ice and frazil horizons observed at M and BM. Figure 18 illustrates the cross-sectional area of the dam at each section as a function of time. These measurements show a pattern of growth and decay similar to those observed in 1983/84 and 1984/85.

Additional frazil dam profiles were obtained at AM and X1 (Figs. 19 and 20). The X1 profile is especially interesting, as it illustrates the rapid changes that can occur in the vicinity of an ice front. The advancing ice front had reached the vicinity of X1 on November 28. The first profile, which was obtained on December 2 when the ice front was only 150 m upstream and the ice only 0.2 m thick, displays the greatest volume of frazil deposition, showing how rapidly such features may form. Most noticeable in subsequent profiles is the rapid erosion that took place at X1 in comparison to the relatively stable frazil dams located at other sections.

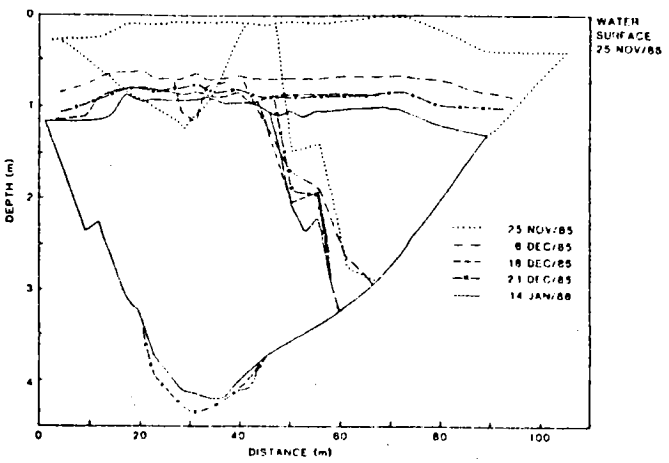

Figure 16. Frazil dam profiles on specific dates at M.

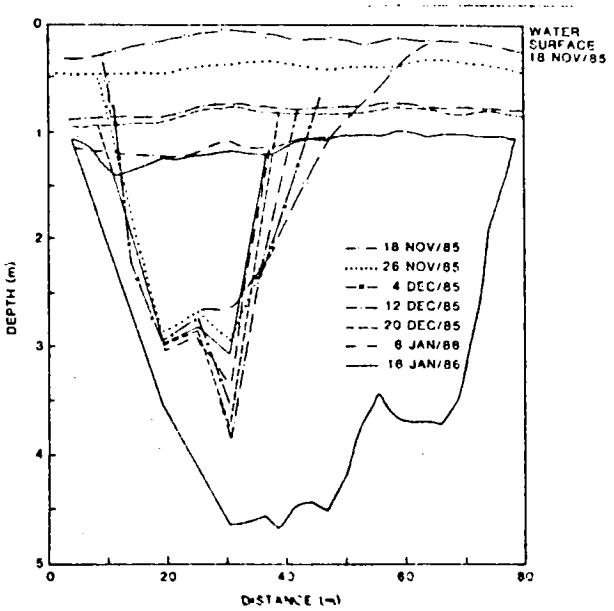

Figure 17. Frazil dam profiles on specific dates at BM.

Table 3. Comparison of the Duration of Ice Cover at BM, M, and AM for Each of the Three Study Years

	1983/84			1984/85			1985/86		
Station	Freeze-up	Breakup	Days	Freeze-up	Breakup	Days	Freeze-up	Breakup	Days
BM	Dec. 4	Mar. 29	115	Dec. 9	Apr. 12	124	Nov. 11	Apr. 22	162
M	Dec. 9	Mar. 25	106	Dec. 13	Apr. 10	118	Nov. 17	Apr. 19	153
AM	Jan. 2	Mar. 23	80	Dec. 29	Apr. 8	100	Dec. 24	Apr. 18	115

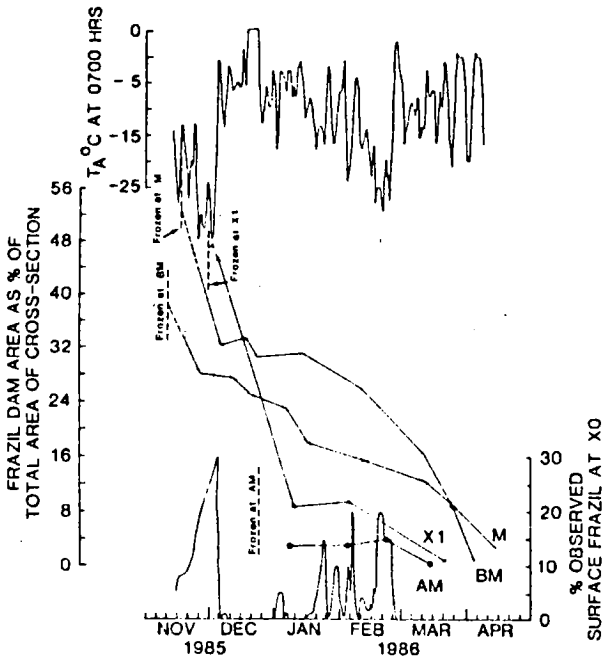

Figure 18. Cross-sectional area as percentage of total frazil dam at AM, M, BM, and X1, air temperature, and percentage observed surface frazil at X0 as functions of time. (T_a refers to air temperature.)

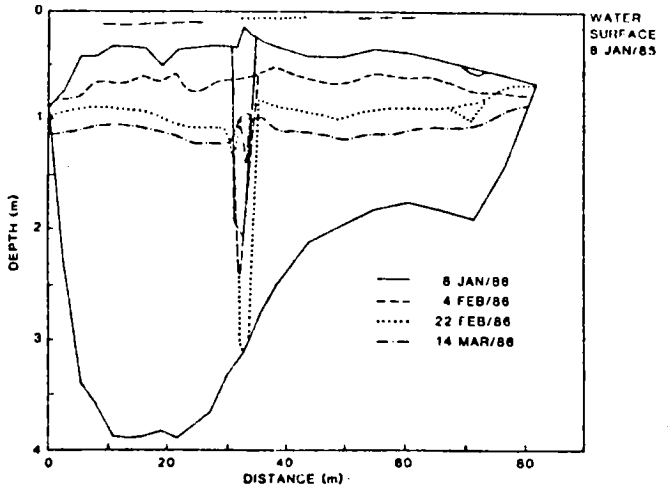

Figure 19. Frazil dam profiles on specific dates at AM.

A summary map of the frazil dam distribution is shown in Figure 21. These data show the dam to be continuous along the reach, to occupy a volume roughly equal to that of sheet ice, and to lie on one side or the other of the axis of maximum flow velocity, which we define as the velocity core. A schematic drawing (Fig. 22) shows the complex distribution of the frazil dam in relation to channel geometry within the vicinity of BM.

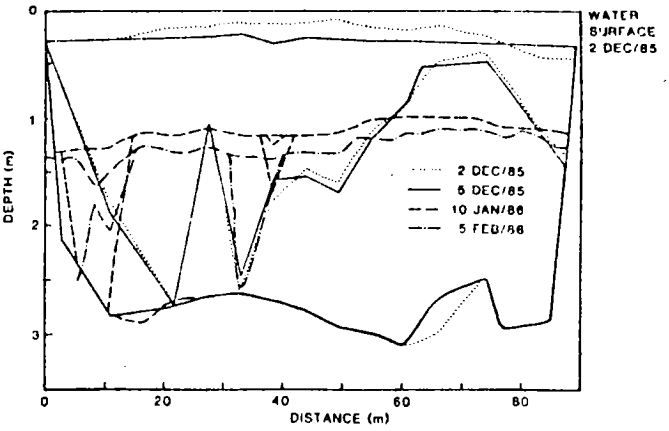

Figure 20. Frazil dam profiles on specific dates at X1.

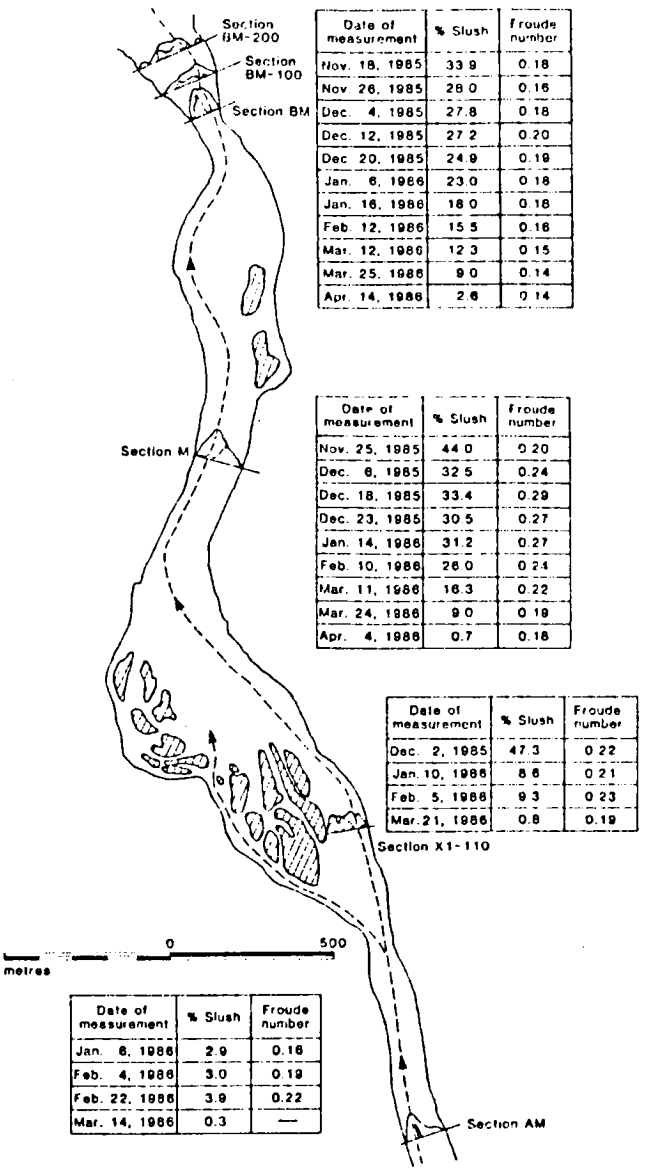

Date of measurement	% Slush	Froude number
Nov. 18, 1985	33.9	0.18
Nov. 26, 1985	28.0	0.16
Dec. 4, 1985	27.8	0.18
Dec. 12, 1985	27.2	0.20
Dec. 20, 1985	24.9	0.19
Jan. 6, 1986	23.0	0.18
Jan. 16, 1986	18.0	0.18
Feb. 12, 1986	15.5	0.16
Mar. 12, 1986	12.3	0.15
Mar. 25, 1986	9.0	0.14
Apr. 14, 1986	2.6	0.14

Date of measurement	% Slush	Froude number
Nov. 25, 1985	44.0	0.20
Dec. 6, 1985	32.5	0.24
Dec. 18, 1985	33.4	0.29
Dec. 23, 1985	30.5	0.27
Jan. 14, 1986	31.2	0.27
Feb. 10, 1986	26.0	0.24
Mar. 11, 1986	16.3	0.22
Mar. 24, 1986	9.0	0.19
Apr. 4, 1986	0.7	0.18

Date of measurement	% Slush	Froude number
Dec. 2, 1985	47.3	0.22
Jan. 10, 1986	8.6	0.21
Feb. 5, 1986	9.3	0.23
Mar. 21, 1986	0.8	0.19

Date of measurement	% Slush	Froude number
Jan. 6, 1986	2.9	0.18
Feb. 4, 1986	3.0	0.19
Feb. 22, 1986	3.9	0.22
Mar. 14, 1986	0.3	—

Figure 21. Frazil dam deposition within the study reach.

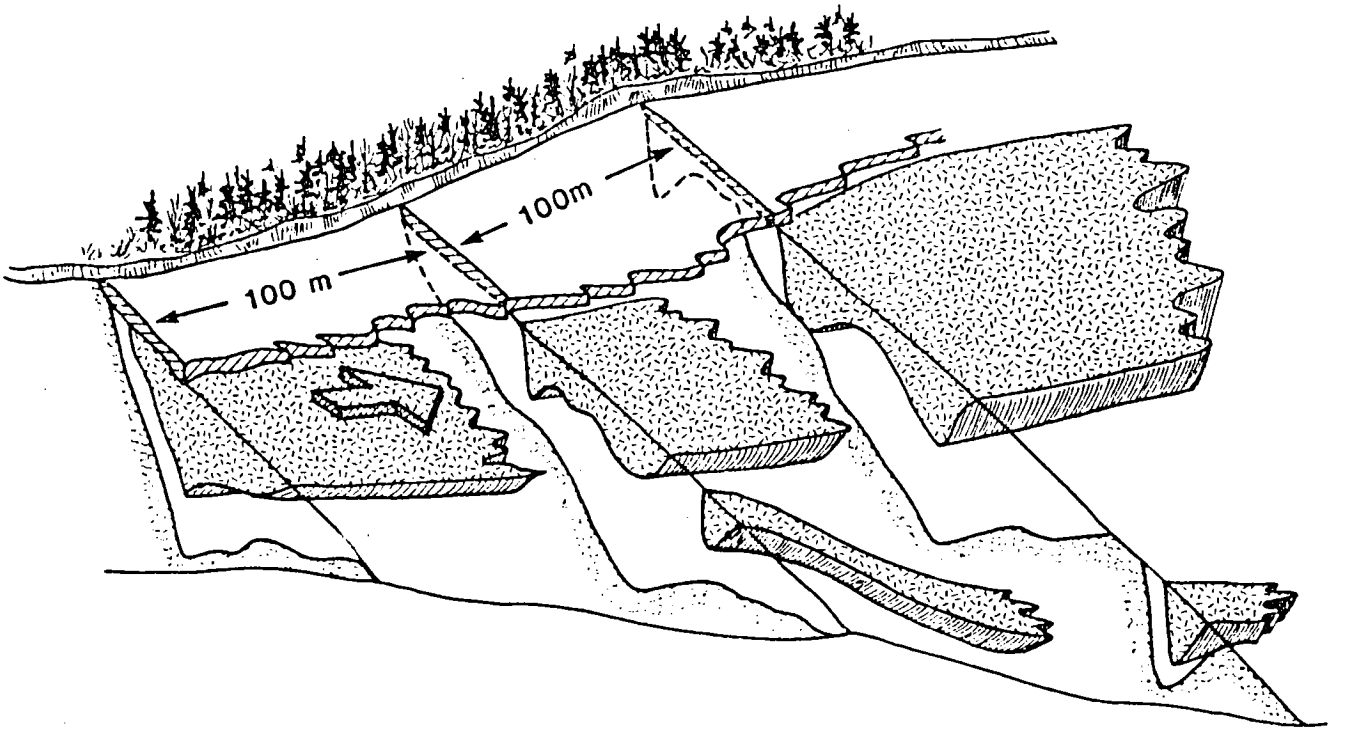

Figure 22. Schematic of frazil dam in a 200-m long section near BM.

Hydraulic Conditions

Observations of water level were recorded daily throughout the winter at X0, AM, M, and BM, and for a short period during freeze-up at X4.

During freeze-up, the hydraulic resistance of a river generally increases requiring a corresponding increase in the depth of flow. Similarly, the overall resistance decreases subsequent to breakup. These effects on resistance are evident from the water level data (Fig. 23, Table 4). Water levels at all stations increased rapidly at freeze-up, declined gradually during winter, and fell sharply following breakup. Similarly, observations of surface slope (Fig. 24) reveal significant variations throughout the winter, with large slopes and rapid variations occurring at freeze-up. Also shown are the large variations in slope accompanying the midwinter occurrence of overflow between X0 and AM.

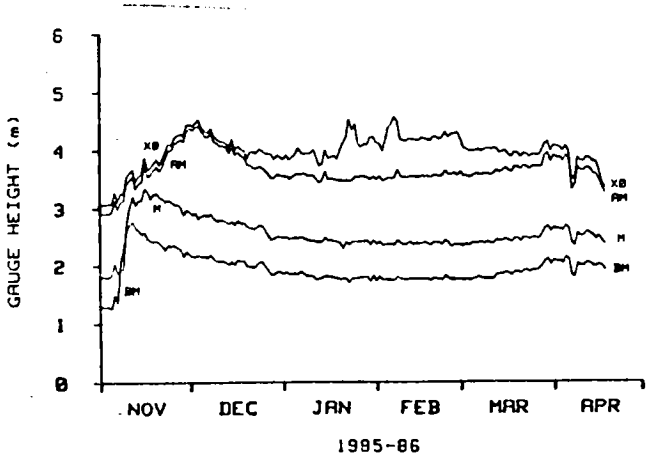

Figure 23. Water levels versus time.

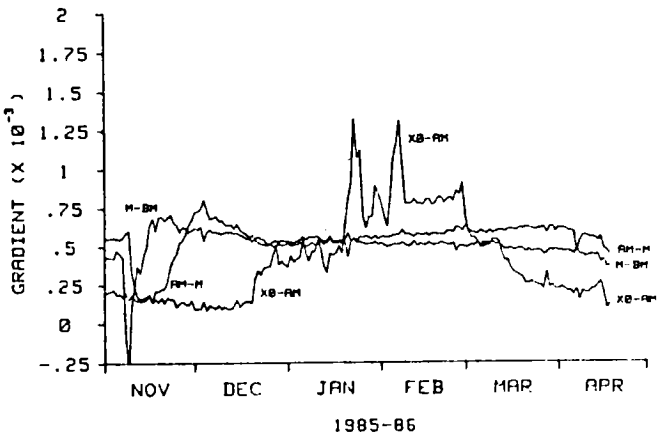

Figure 24. Surface slopes versus time.

Table 4. Daily Values of Streamflow (Q) and Water Level (relative to Geodetic Datum) during the Winter of 1985/86

Date	Q ($m^3 s^{-1}$)	X0 (m)	AM (m)	M (m)	BM (m)
85-10-31	137	630.785	630.630	–	–
85-11-01	144	630.725	630.570	629.475	628.958
85-11-04	140	630.745	630.570	629.458	628.951
85-11-05	143	630.745	630.600	629.498	628.928
85-11-06	137	630.945	630.790	629.698	629.158
85-11-07	137	630.785	630.650	629.538	629.028
85-11-08	148	630.925	630.770	629.598	629.709
85-11-09	134	630.920	630.800	629.598	629.936
85-11-10	139	631.215	631.070	630.411	630.273
85-11-11	138	631.285	631.160	630.681	630.390
85-11-12	140	631.335	631.220	630.871	630.428
85-11-13	139	631.130	631.000	630.711	630.325
85-11-14	140	631.225	631.095	630.801	630.282
85-11-15	139	631.265	631.125	630.811	630.218
85-11-16	141	631.535	631.390	631.011	630.245
85-11-17	137	631.335	631.220	630.951	630.132
85-11-18	140	631.365	631.240	630.821	630.099
85-11-19	140	631.435	631.325	630.911	630.085
85-11-20	139	631.515	631.380	630.931	630.097
85-11-21	137	631.415	631.310	630.861	630.059
85-11-22	138	631.515	631.380	630.831	630.006
85-11-23	137	631.645	631.520	630.781	629.933
85-11-24	136	631.775	631.650	630.811	630.023
85-11-25	137	631.755	631.670	630.771	630.003
85-11-26	137	631.885	631.780	630.731	630.018
85-11-27	135	631.925	631.810	630.731	629.978
85-11-28	135	631.950	631.850	630.691	629.948
85-11-29	131	631.915	631.820	630.541	629.828
85-11-30	137	632.100	631.980	630.636	629.908
85-12-01	135	632.125	632.050	630.601	629.858
85-12-02	135	632.085	632.010	630.551	629.818
85-12-03	134	632.145	632.070	630.581	629.828
85-12-04	134	632.205	632.090	630.481	629.838
85-12-05	134	632.065	632.000	630.531	629.818
85-12-06	135	632.005	631.910	630.551	629.818
85-12-07	134	631.975	631.890	630.521	629.808
85-12-08	134	632.045	631.970	630.571	629.858
85-12-09	135	631.915	631.820	630.486	629.778
85-12-10	133	631.865	631.790	630.446	629.748
85-12-11	133	631.825	631.740	630.451	629.738
85-12-12	131	631.815	631.740	630.461	629.748
85-12-13	132	631.795	631.720	630.431	629.718
85-12-14	131	631.710	631.620	630.391	629.688
85-12-15	129	631.865	631.740	630.441	629.733
85-12-16	133	631.675	631.590	630.371	629.678
85-12-17	128	631.745	631.640	630.451	629.768
85-12-18	126	631.685	631.570	630.401	629.738
85-12-19	124	631.655	631.540	630.411	629.748
85-12-20	124	631.525	631.420	630.351	629.658
85-12-21	128	631.635	631.410	630.321	629.658
85-12-22	128	631.645	631.370	630.311	629.633
85-12-23	129	631.610	631.355	630.321	629.658
85-12-24	134	631.685	631.395	630.371	629.718
85-12-25	132	631.665	631.370	630.361	629.738
85-12-26	132	631.615	631.320	630.281	629.658

Table 4. Continued

Date	Q ($m^3 s^{-1}$)	X0 (m)	AM (m)	M (m)	BM (m)
85-12-27	132	631.615	631.260	630.191	629.588
85-12-28	130	631.595	631.190	630.111	629.508
85-12-29	130	631.505	631.200	630.141	629.518
85-12-30	133	631.585	631.260	630.171	629.558
85-12-31	129	631.545	631.240	630.171	629.558
86-01-01	130	631.515	631.220	630.151	629.523
86-01-02	133	631.585	631.230	630.171	629.558
86-01-03	129	631.500	631.180	630.131	629.518
86-01-04	130	631.545	631.210	630.141	629.528
86-01-05	130	631.595	631.250	630.161	629.528
86-01-06	130	631.705	631.270	630.141	629.518
86-01-07	126	631.625	631.260	630.171	629.568
86-01-08	124	631.595	631.270	630.141	629.528
86-01-09	123	631.615	631.240	630.121	629.488
86-01-10	131	631.605	631.230	630.101	629.488
86-01-11	127	631.675	631.240	630.106	629.483
86-01-12	125	631.555	631.170	630.081	629.428
86-01-13	121	631.405	631.110	630.081	629.438
86-01-14	126	631.425	631.160	630.081	629.453
86-01-15	128	631.665	631.300	630.161	629.488
86-01-16	123	631.525	631.170	630.101	629.478
86-01-17	127	631.545	631.180	630.111	629.478
86-01-18	124	631.575	631.170	630.091	629.458
86-01-19	127	631.515	631.150	630.081	629.448
86-01-20	122	631.665	631.150	630.061	629.428
86-01-21	125	631.785	631.140	629.961	629.244
86-01-22	123	631.875	631.150	630.081	629.442
86-01-23	123	632.195	631.140	630.031	629.374
86-01-24	124	632.005	631.150	630.081	629.448
86-01-25	122	632.105	631.210	630.081	629.444
86-01-26	119	631.755	631.200	630.081	629.454
86-01-27	126	631.715	631.220	630.081	629.464
86-01-28	123	631.765	631.210	630.091	629.468
86-01-29	122	631.755	631.200	630.101	629.478
86-01-30	120	631.875	631.160	630.021	629.384
86-01-31	127	631.885	631.210	630.111	629.494
86-02-01	121	631.785	631.160	630.031	629.404
86-02-02	119	631.775	631.220	630.091	629.478
86-02-03	118	631.645	631.140	630.021	629.424
86-02-04	119	631.805	631.160	630.031	629.424
86-02-05	118	632.045	631.190	630.041	629.424
86-02-06	118	632.105	631.180	–	–
86-02-07	118	632.235	631.190	630.031	629.414
86-02-08	120	632.155	631.330	630.111	629.478
86-02-09	122	631.835	631.210	630.051	629.438
86-02-10	108	631.825	631.200	630.031	629.428
86-02-11	117	631.815	631.190	630.051	629.428
86-02-12	117	631.855	631.210	630.081	629.438
86-02-13	109	631.835	631.210	630.041	629.438
86-02-14	113	631.835	631.210	630.051	629.428
86-02-15	115	631.815	631.200	630.051	629.438
86-02-16	116	631.865	631.220	630.051	629.438
86-02-17	116	631.855	631.210	630.071	629.438
86-02-18	117	631.835	631.220	630.051	629.438
86-02-19	113	631.815	631.190	630.021	629.408

Table 4. Continued

Date	Q ($m^3 s^{-1}$)	X0 (m)	AM (m)	M (m)	BM (m)
86-02-20	115	631.885	631.230	630.071	629.453
86-02-21	115	631.885	631.230	630.071	629.438
86-02-22	113	631.835	631.210	630.061	629.438
86-02-23	113	631.875	631.230	630.031	629.418
86-02-24	110	631.965	631.310	630.111	629.498
86-02-25	110	631.875	631.240	630.061	629.438
86-02-26	111	631.935	631.245	629.991	629.428
86-02-27	112	631.935	631.270	630.031	629.428
86-02-28	111	631.960	631.230	630.031	629.428
86-03-01	110	631.845	631.290	630.021	629.428
86-03-02	111	631.695	631.220	630.011	629.418
86-03-03	113	631.670	631.225	630.041	629.428
86-03-04	105	631.640	631.195	630.021	629.418
86-03-05	108	631.645	631.220	630.061	629.428
86-03-06	110	631.645	631.255	630.051	629.448
86-03-07	109	631.665	631.245	630.061	629.473
86-03-08	109	631.635	631.235	630.076	629.448
86-03-09	106	631.665	631.260	630.051	629.438
86-03-10	106	631.685	631.250	630.081	629.448
86-03-11	105	631.675	631.240	630.051	629.438
86-03-12	108	631.685	631.260	630.051	629.438
86-03-13	105	631.685	631.320	630.111	629.513
86-03-14	112	631.605	631.280	630.091	629.518
86-03-15	111	631.635	631.310	630.096	629.518
86-03-16	110	631.645	631.360	630.131	629.548
86-03-17	109	631.575	631.310	630.101	629.533
86-03-18	110	631.535	631.280	630.071	629.498
86-03-19	113	631.615	631.370	630.131	629.548
86-03-20	109	631.605	631.370	630.141	629.563
86-03-21	111	631.535	631.330	630.081	629.528
86-03-22	111	631.595	631.390	630.151	629.578
86-03-23	114	631.585	631.370	630.141	629.588
86-03-24	109	631.535	631.330	630.121	629.558
86-03-25	115	631.575	631.380	630.151	629.588
86-03-26	115	631.575	631.380	630.151	629.588
86-03-27	126	631.555	631.380	630.131	629.598
86-03-28	130	631.635	631.370	630.201	629.658
86-03-29	127	631.745	631.560	630.311	629.738
86-03-30	132	631.805	631.610	630.351	629.788
86-03-31	138	631.625	631.450	630.261	629.688
86-04-01	139	631.735	631.560	630.321	629.758
86-04-02	139	631.715	631.530	630.301	629.738
86-04-03	139	631.705	631.530	630.301	629.748
86-04-04	136	631.635	631.470	630.271	629.708
86-04-05	146	631.725	631.560	630.361	629.808
86-04-06	147	631.635	631.490	630.311	629.778
86-04-07	142	631.165	630.990	630.061	629.488
86-04-08	114	631.175	631.060	630.001	629.468
86-04-09	121	631.525	631.360	630.231	629.698
86-04-10	129	631.465	631.310	630.171	629.658
86-04-11	131	631.465	631.310	630.191	629.668
86-04-12	135	631.535	631.360	630.251	629.718
86-04-13	134	631.515	631.340	630.231	629.708
86-04-14	131	631.455	631.260	630.191	629.658
86-04-15	132	631.405	631.240	630.121	629.648

Table 4. Continued

Date	Q ($m^3 s^{-1}$)	X0 (m)	AM (m)	M (m)	BM (m)
86-04-16	135	631.305	631.150	630.181	629.688
86-04-17	135	631.105	631.030	630.091	629.658
86-04-18	150	631.015	630.920	630.031	629.588

The dominating influence of ice front position on water levels (the so-called backwater effect) is shown in Figure 25. In Figure 26, the water level at AM is plotted against the position of the ice front within the reach. Note that a slight backwater effect occurs as the ice front passes

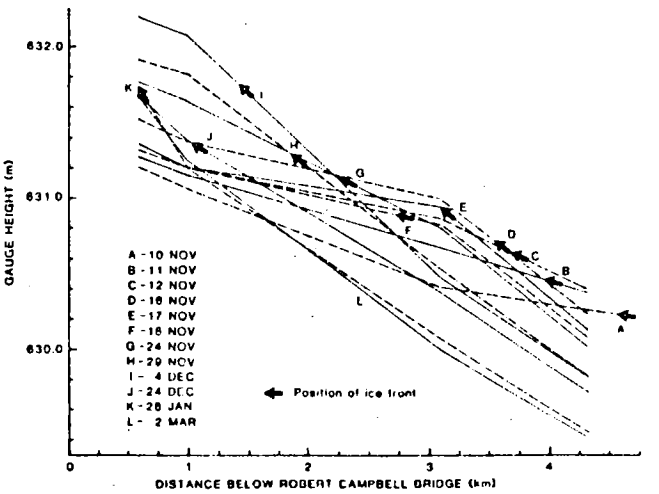

Figure 25. Surface slopes within the reach at selected times.

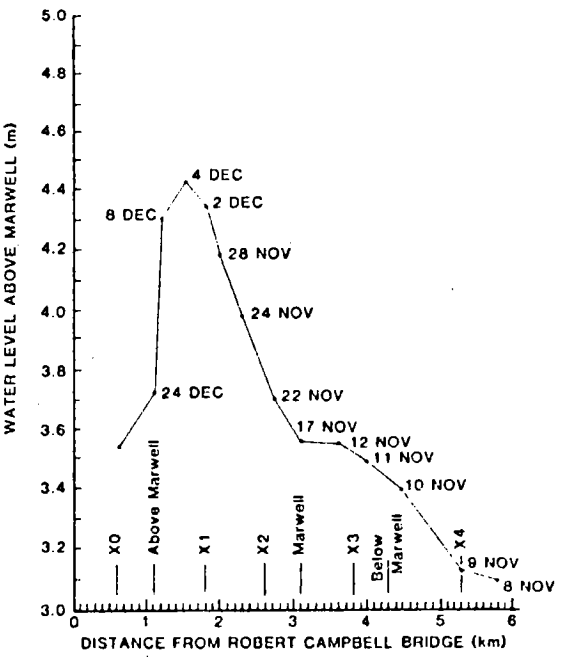

Figure 26. Ice front position versus water level at AM.

BM, and that a much larger effect occurs as the front reaches the vicinity of X2. This response is relevant to concerns for flooding and dam operation.

PROCESS-RELATED OBSERVATIONS

Water Temperature Changes at Freeze-up

Changes in water temperature along the reach at different times during freeze-up are shown in Figure 27. Typically, the temperature changes by 0.2°C to 0.3°C between the bridge and BM, yielding a longitudinal temperature gradient dT/dL = 0.05-0.07°C/km. This gradient can be used to estimate the rate of cooling within the reach. By taking the mean velocity $\langle V \rangle = 0.7$ m s^{-1}, we note that a column of water moving through the reach cools at a rate of $dT/dt = \langle V \rangle dT/dL$, or between 0.3 to 0.5 x 10^{-4}°C s^{-1}. Taking the mean depth of the reach to be 2 m, a surface heat flux of 260 to 390 W m^{-2} is obtained. This should be considered as a rough estimate only, but is in agreement with previous heat flux measurements (Alford and Carmack, 1987a), and is similar to observations from 1984/85.

Edge Ice Growth

Generally, freeze-up is characterized by a gradual closing in of edge ice forming a narrow channel along the velocity core, coupled with a progressive advance of the ice front due to the deposition of floes formed farther upstream. Osterkamp and Gosink (1983) say that edge ice grows laterally by conductive heat transfer through the ice, by the accumulation of drifting frazil, and by loss of latent heat to supercooled river water. In 1985/86, however, edge ice did not develop in a manner allowing long-term study. That is, because of fluctuating air temperatures and frequent inundation, the edge ice either formed and broke away, or was buried by freezing overflow. Because of these limitations, the rate of edge ice growth was observed at M for only an 8-day period (Fig. 28). These data show only a weak relationship to air temperature.

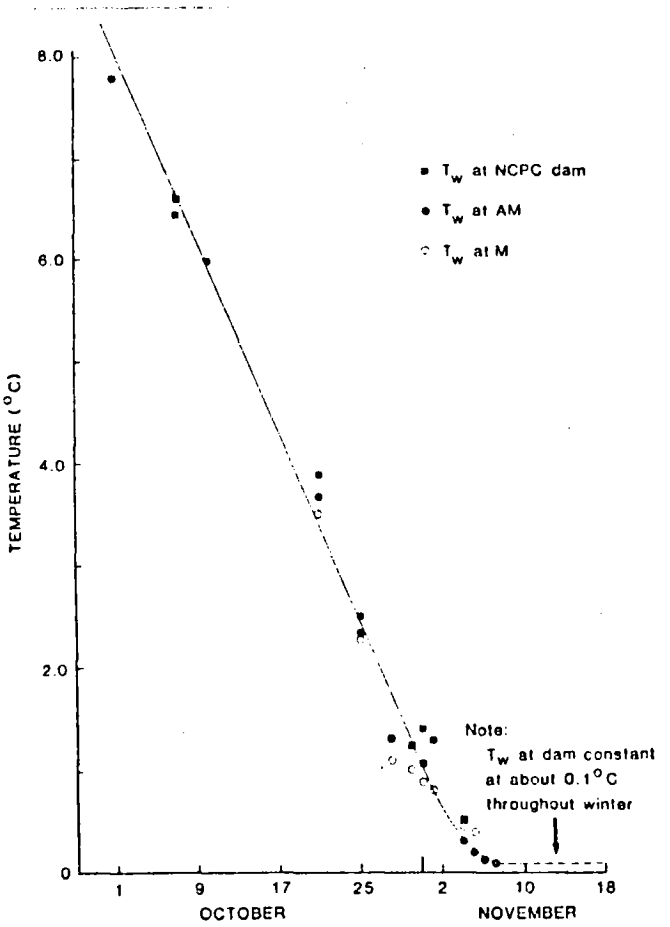

Figure 27. Water temperature along reach during freeze-up (T_w refers to water temperature; T_a refers to air temperature.)

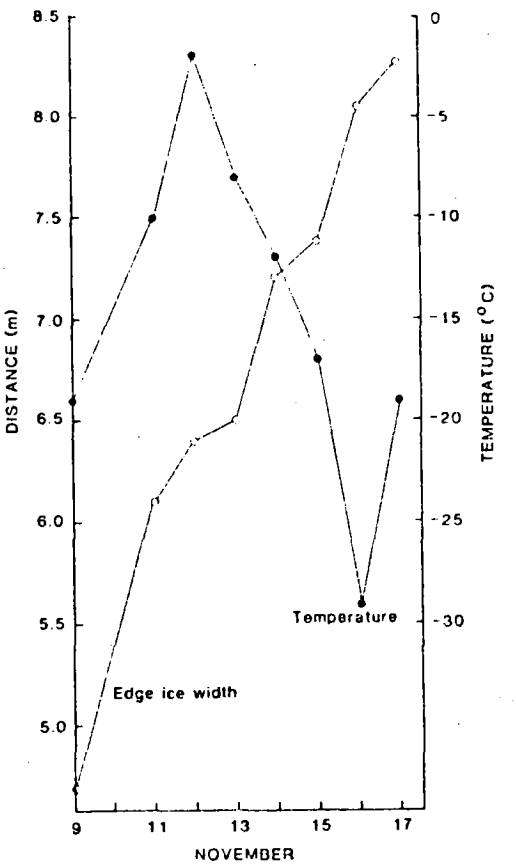

Figure 28. Edge ice width and air temperature versus time.

Ice Front Advance

The rate of ice front advance through the reach is of prime engineering concern, for it is during this time that the Marwell region of Whitehorse is most prone to flooding. It was noted above that the backwater effect increased as the ice front passed X2, suggesting that the sensitivity of flooding is related to the speed of ice front advance.

Observations of ice front advance through the reach were made in 1983/84, 1984/85, and 1985/86 (Fig. 29). In general, it appears that the ice front propagates very quickly from X4 to X2, slows between X2 and X1, and moves very slowly above X1.

Admittedly, the prevailing air temperatures have the greatest effect on the winter regime of the river, but in ways that are sometimes unexpected. This was brought in very clear perspective during 1985/86 when drastic reversals in weather patterns were experienced. Coincident with cold weather and the formation of much frazil and anchor ice, the ice front passed rapidly from X4 to just downstream from AM as expected. What was difficult to foresee was the subsequent effect of warm temperatures on water levels and the flooding of the existing ice cover. Fluctuations in water level resulted in considerable edge ice breaking loose and floating into the open parts of the reach. These would then lodge at the ice front to extend it upstream at a very rapid rate. This is what happened between AM and the Robert Campbell Bridge.

Ice Ripple Formation

Past research has shown that, with the onset of spring, instabilities in the flow of water warmer than the freezing temperature can result in the formation of wavelike features, called ice ripples, at the icewater interface (Carey, 1966; Ashton and Kennedy, 1972). The fluid mechanics of heat transfer at an ice/water interface in the presence of turbulent flow has been treated by Gilpin *et al.* (1980). It has been noted (Alford and Carmack, 1987a) that the hydraulic resistance of the reach appeared to increase coincident with the onset of ripple formation.

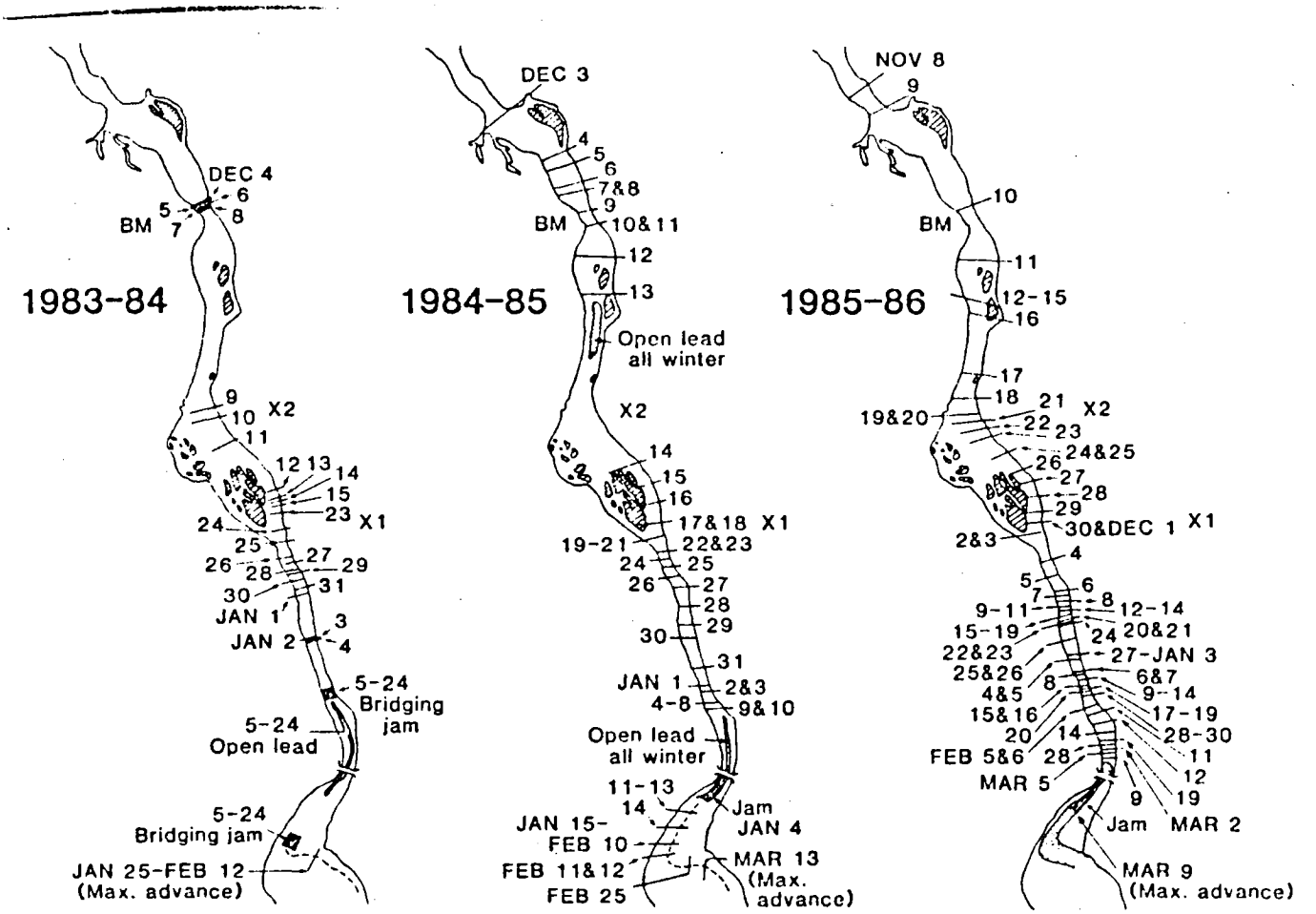

Figure 29. Comparison of ice front advance during the three winters of study.

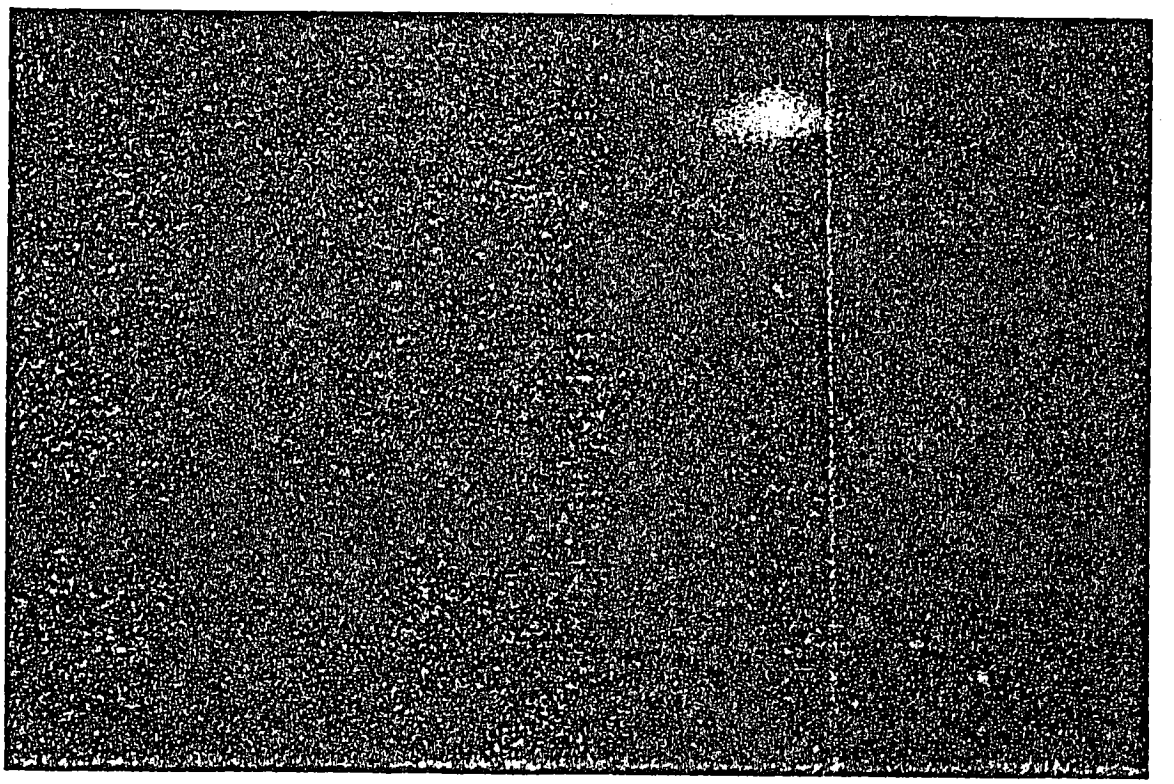

(a) March 19.

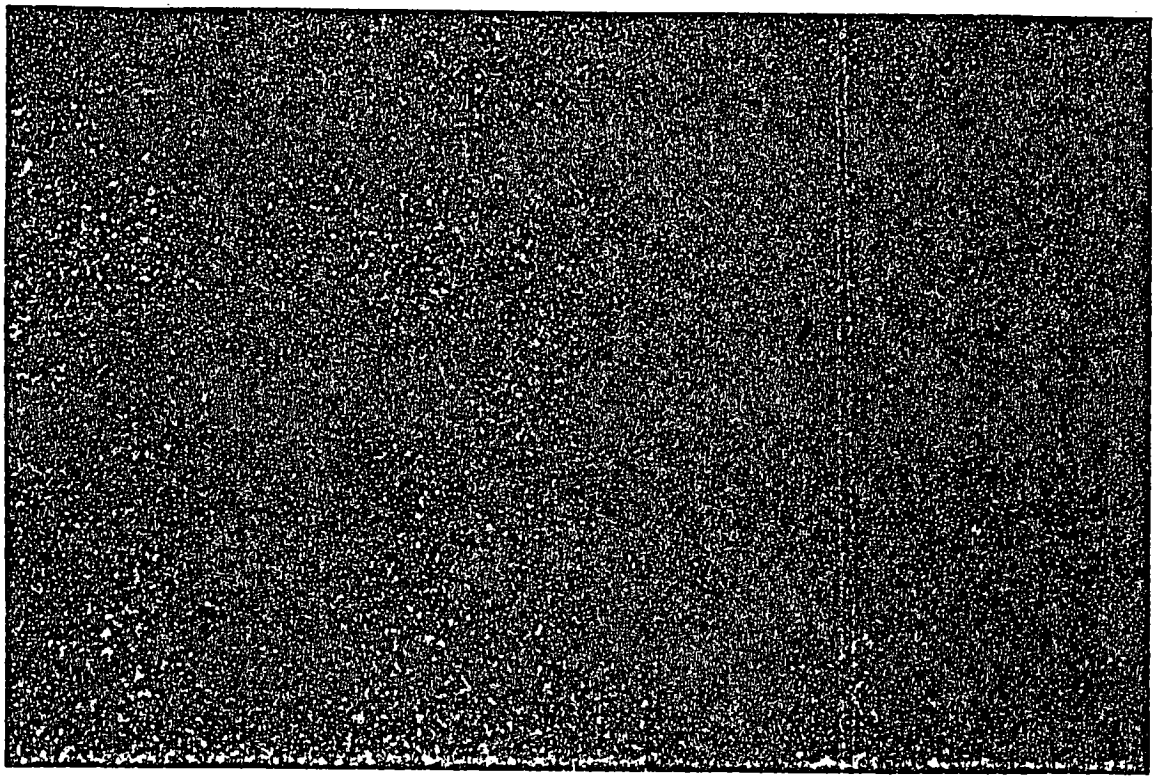

(b) March 24.

Figure 30. Plan view of the underside of ice blocks showing the progressive development of ice ripples on specific dates.

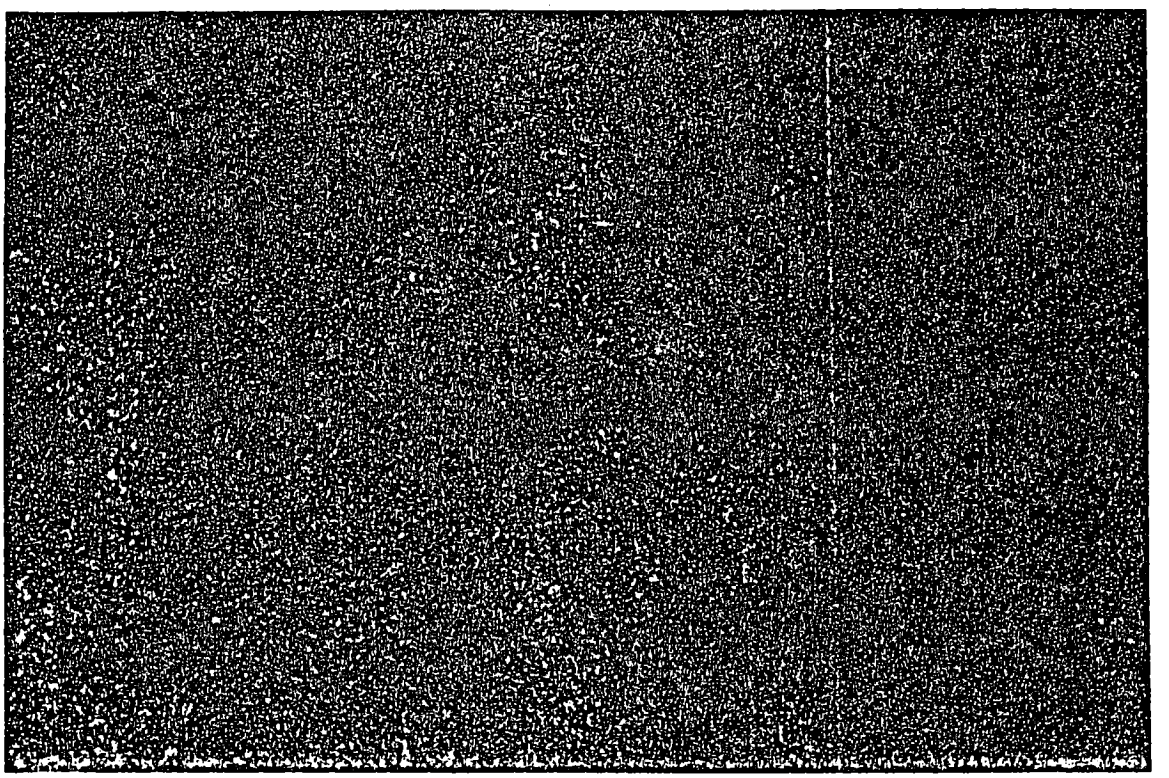

(c) March 29.

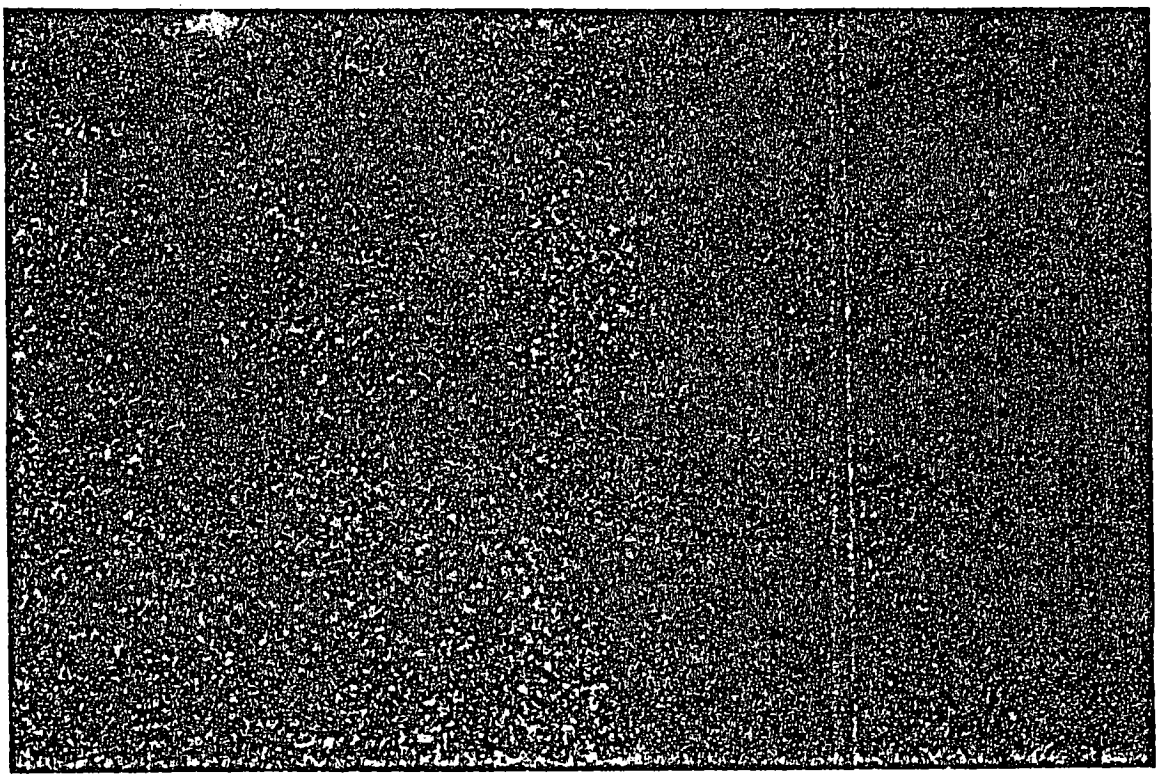

(d) April 3.

(e) April 9.

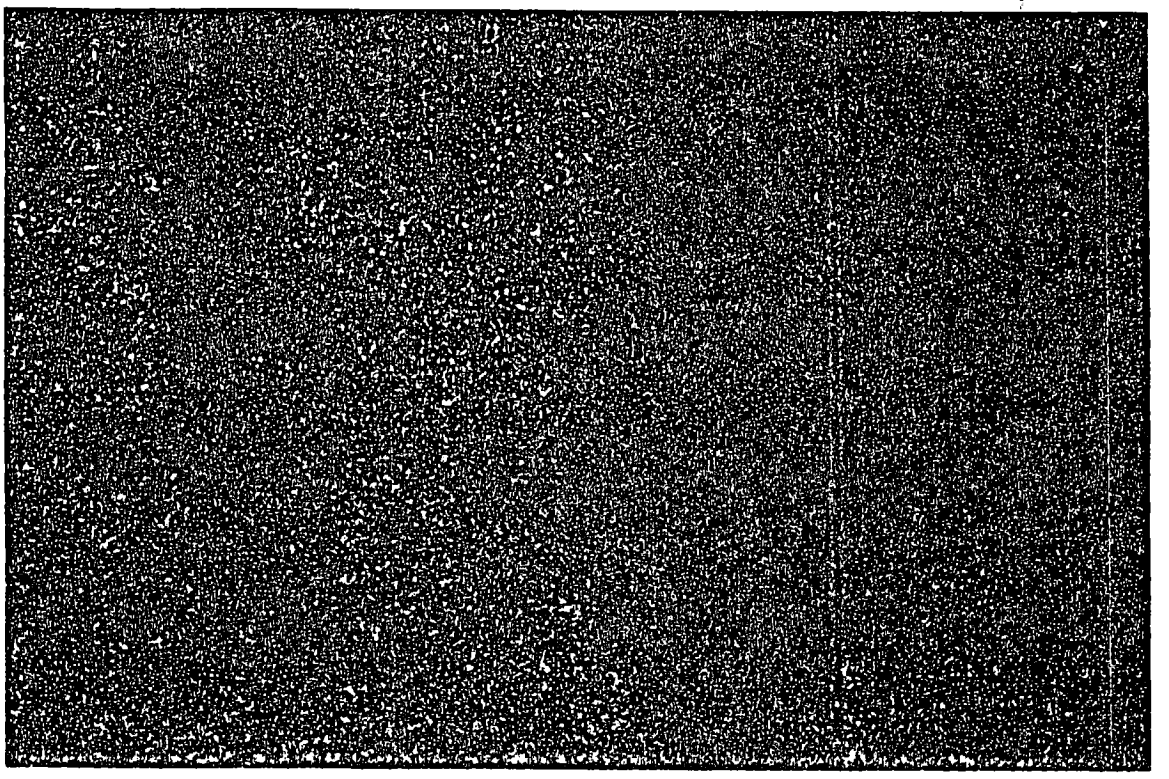

(f) April 15.

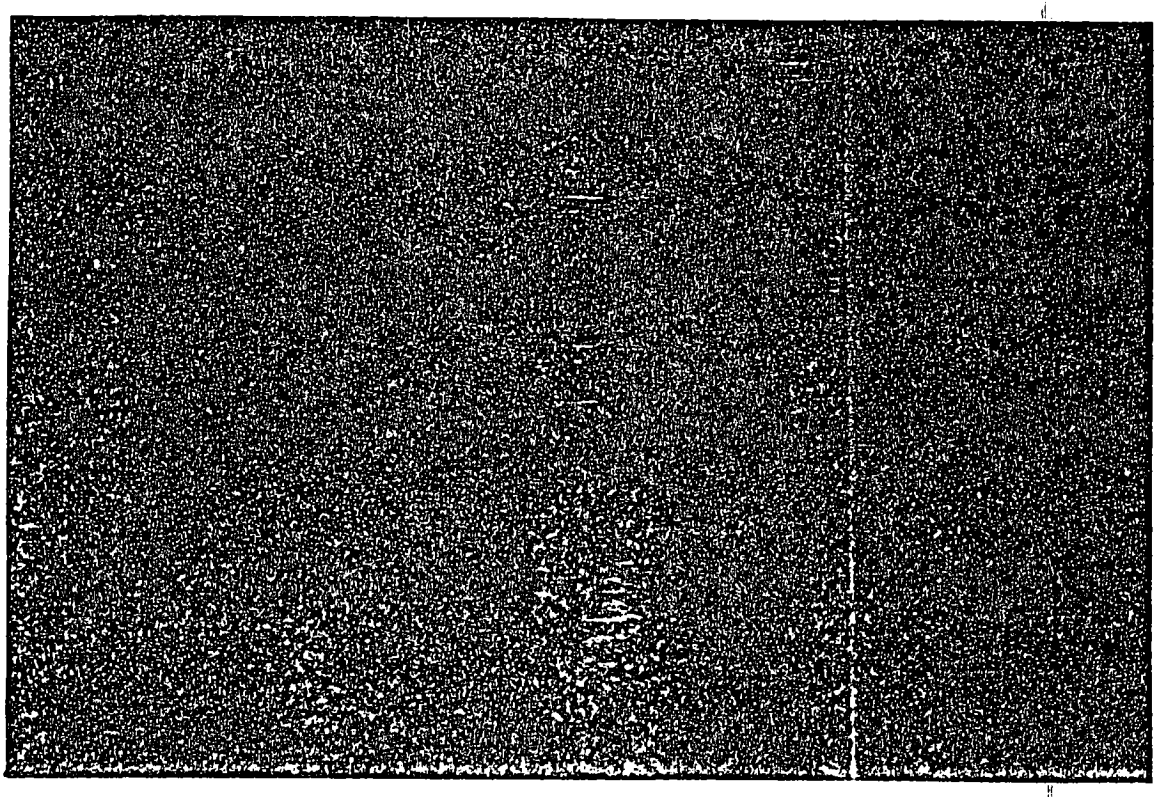

(a) March 10.

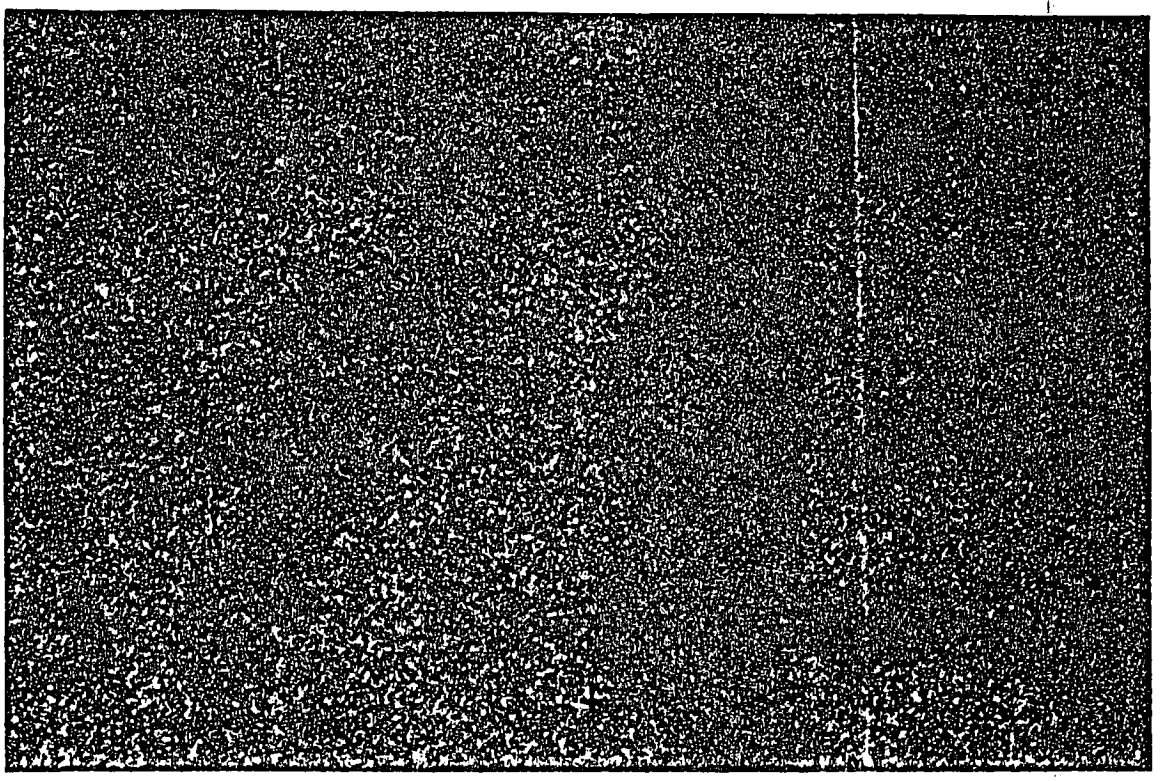

(b) April 15.

Figure 31. Side view of the underside of ice blocks showing the transition from a flat surface on March 10 to the time of maximum ripple amplitude on April 15.

In general, the development of ripples followed the same pattern in 1986 as in 1985; namely, dramatic changes in the texture of the ice/water interface occurred in a very short period of time, as shown in Figures 30 and 31. Initially, the bottom of the ice was featureless; then, as solar radiation began to penetrate the cover and warm the underlying water, ripples began to form. Initially the ripples were essentially straight-crested with wavelengths of about 0.10 m and amplitudes of about 0.01 m. As the amplitudes of the ripples grew to about 0.02 m, secondary points of instability and melting appeared, and the wave crests began to undulate. In the final stages, the crests of the ripples became discontinuous and broken and thus could not be traced over distances much longer than the wavelength. By this time the amplitudes were of order 0.05 m. Figure 32 shows water level, air temperature, and streamflow attendant to the period of ripple formation and breakup.

Two new aspects associated with the formation of ripples were observed in 1986. The first concerned their development in midwinter. During an inspection on December 21 of the isolated ice cover that extended above the Robert Campbell Bridge, it was observed that one of the pans that had lodged at the ice front had inverted to expose a rippled undersurface (see Fig. 10). It is likely that this block had its origin as edge ice in that reach of the river close to the hydro dam outfall where water temperatures are highest. Such an observation clearly shows that ripple formation is not only a spring (solar radiation induced) phenomenon, but may develop wherever water temperatures and flow are favourable, e.g., in the proximity of heated outfalls or lake outlets.

The second observation concerns the occurrence and migration of ripples through white ice. Recall that, because

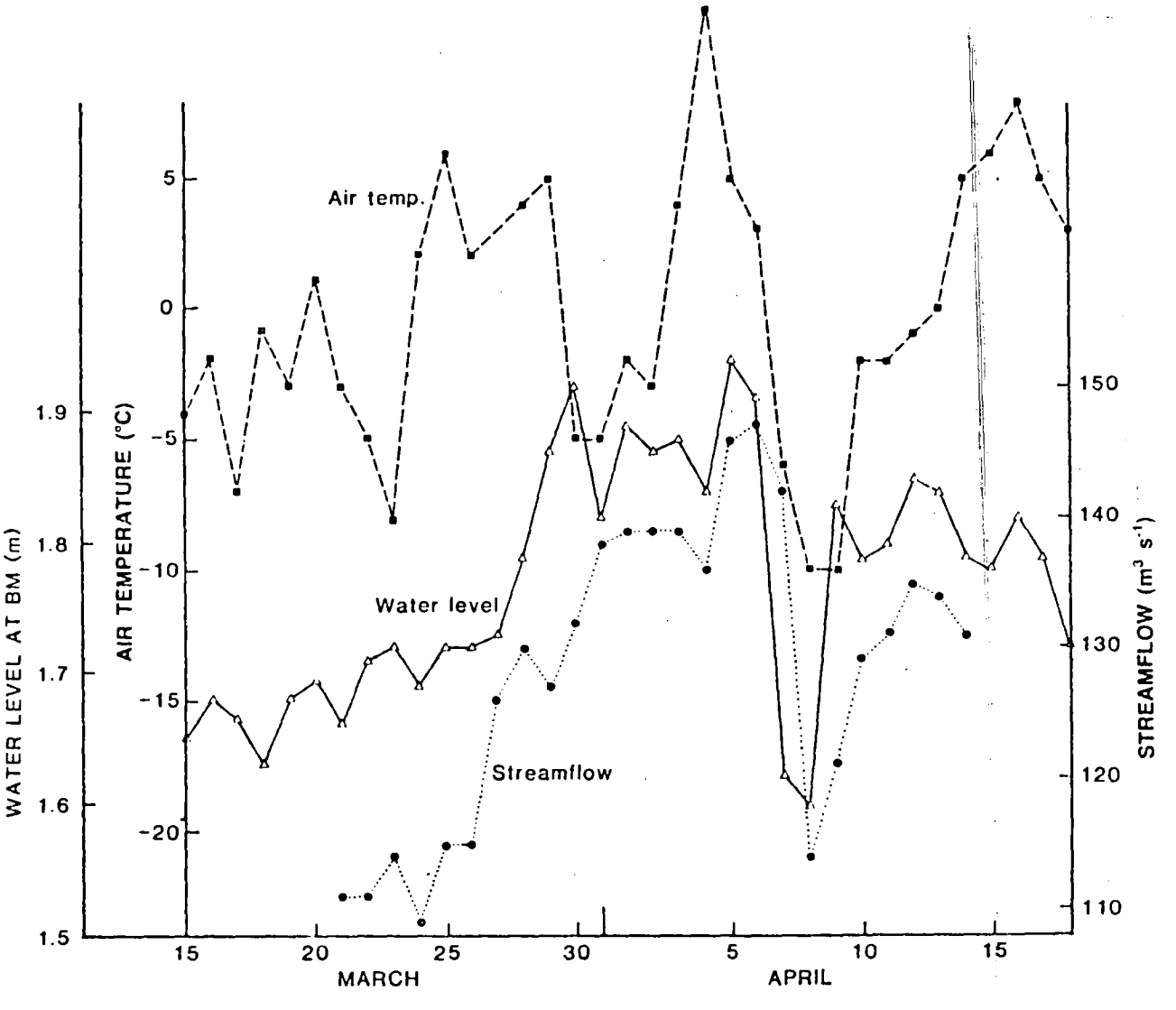

Figure 32. Water level, air temperature, and streamflow during breakup.

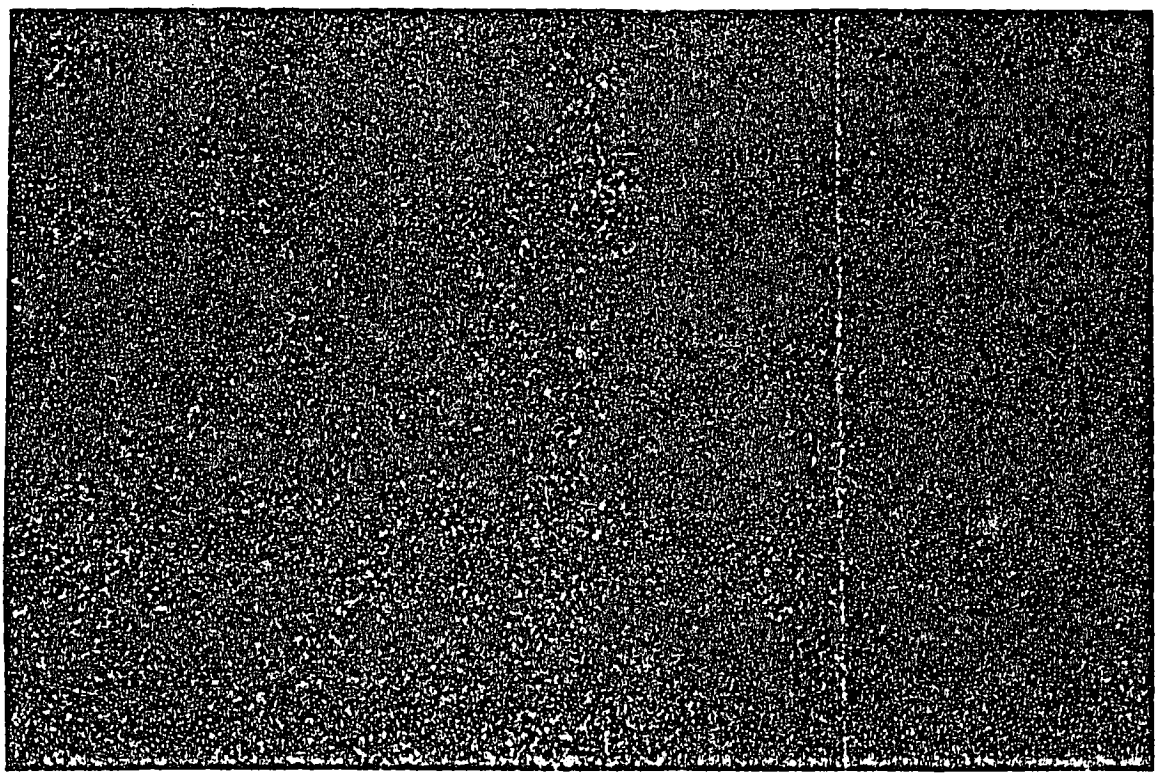

(a) Oblique view.

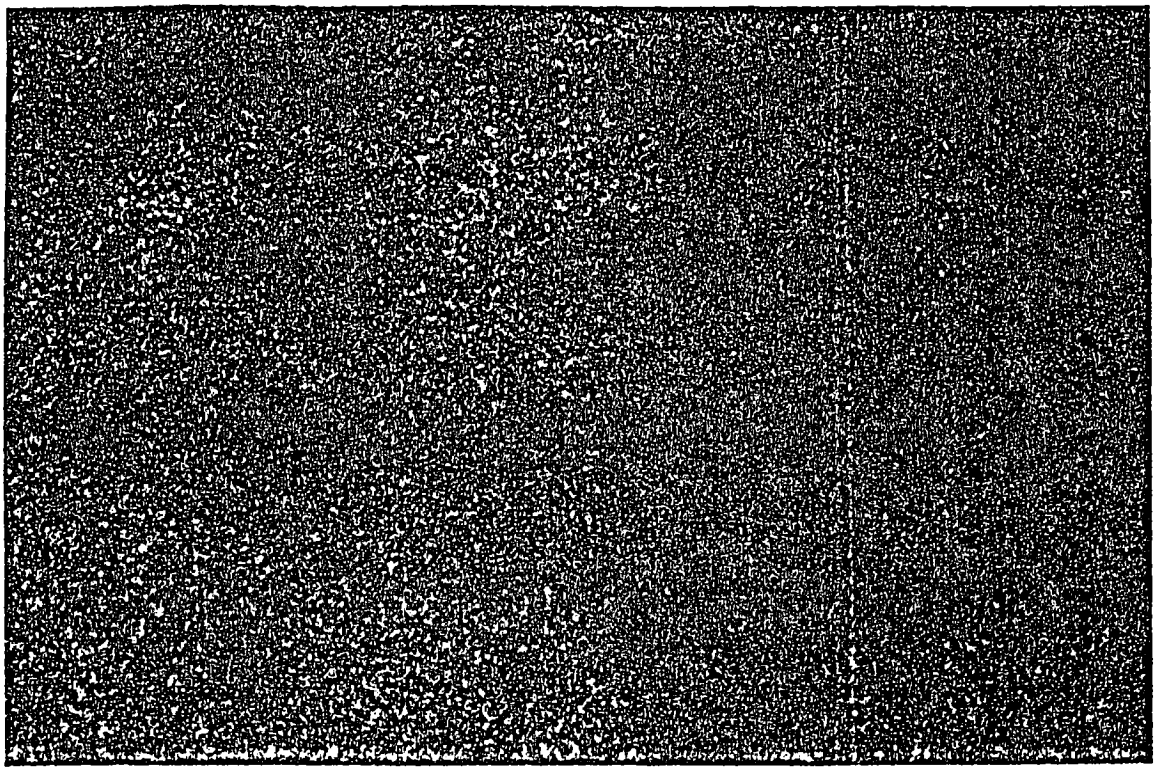

(b) Side view.

Figure 33. Oblique and side views of the underside of white ice at BM on April 21.

of midwinter flooding of the ice and snow cover and subsequent refreezing, the ice between M and AM was layered, with about 0.40 m of white ice overlying 0.40 m of black. That the development of ripples continues to be as much a characteristic feature at the base of melting white ice as well as black ice is shown in Figure 33. In black ice, the ripples were observed to migrate upwards at a rate of about 0.02 m d^{-1}; however, upon reaching the white ice, the migration rate increased to 0.40 m d^{-1}. In fact, the entire layer of white ice vanished in about one day.

The rapid ablation of white ice is a factor that can affect the safety of anyone crossing the ice. In one day the strength of the ice can practically disappear. Further, this occurs by melting from below, with absolutely no noticeable alteration of the ice surface to warn of change.

Analysis of Velocity Profiles

Here, we test a new method of stream gauging in ice-covered rivers that utilizes a single-point measurement of velocity at each vertical in the section.

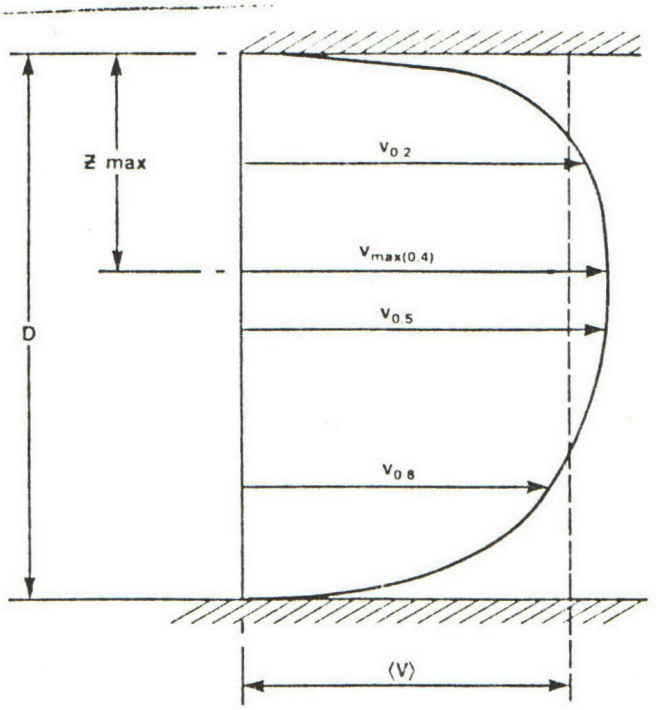

CONVENTIONAL ESTIMATES:

IF D >0.75 m

$\langle V \rangle = (v_{0.2} + v_{0.8}) / 2$

IF D < 0.75 m

$\langle V \rangle = 0.88\ (v_{0.5})$

"486" METHOD

$\langle V \rangle = 0.86\ (v_{0.4})$

Figure 34. Velocity definitions used in the text and methods for estimating mean velocity.

We know from previous enquiry by other investigators and through the observations made during our own program that flow velocity is highly variable in both time and space. A practical problem that follows from this is how to obtain optimum estimates of streamflow from field measurements. To obtain an estimate of the mean velocity for flow under ice cover, the conventional method, used by the Water Survey of Canada, is to average the velocities at the 0.2 and 0.8 depths ($v_{0.2}$ and $v_{0.8}$) or, when the depth is less than 0.75 m, to multiply the velocity at the 0.5 depth ($v_{0.5}$) by the coefficient 0.88 (see Fig. 34). However, an analysis of velocity profiles obtained throughout the winter in 1983/84 (Alford and Carmack, 1987a) revealed that the 0.4 depth was both the mean depth of the maximum velocity and the depth of minimum variance in plots of normalized velocity versus normalized depth. Hence, seasonal changes in the shape of velocity curves associated with ice cover roughness (see Lau, 1982, for complete discussion) are minimized at this depth. This suggests that a single measurement of velocity, observed at the 0.4 depth and multiplied by an appropriate coefficient, can yield an accurate estimate of the mean velocity of the profile. Subsequently, a reevaluation of historical velocity profiles and of data obtained in the YISEX program was carried out. Through mathematical and graphical evaluation (see Papadakis *et al.*, 1987, for details), it was confirmed that the application of a coefficient of 0.86 to velocities observed at the 0.4 depth yielded a value very close to the mean velocity of the full profile. We refer to this as the "486" method, a summary of which is given below.

Basically, then, we will estimate the mean velocity at a given vertical, V, by an algebraic expression $V = R\ v_{max}$, where v_{max} is the maximum velocity. For operational purposes, it is necessary to specify the depth at which v_{max} is most likely to occur; this will be found as $Z_{max} = z_{max}/D$, the normalized depth of the velocity maximum (Fig. 34). Similarly, the coefficient R is the average ratio of the mean velocity to the maximum velocity, or $R = \langle V/v_{max} \rangle$, where the symbol <> is taken to be the average over a large number of vertical profile observations.

Data used in determining the coefficients for the above method are tabulated in Table 5. Ten or more measurements of velocity at each vertical have been fitted to the power-law described in Albord and Carmack (1987a). The first three columns give the location, date, and depth of the station. Column 4 shows whether or not a frazil dam was present. Column 5 lists the normalized depth of the maximum velocity z_{max}/D. Column 6 gives $v_{0.4}$, the velocity at the 0.4 depth, which we show below is the average depth of v_{max}. Column 7 gives the mean velocity V as obtained by numerical integration of the velocity probile; this is taken as the control estimate of the mean velocity. The ratio V/v_{max} is given in column 8.

Table 5. Analysis of Historical Data to Determine Parameters Used in the "486" Method

1	2	3	4	5	6	7	8	9	10
Location	Date	Depth (m)	Ice conditions*	$\frac{z_{max}}{D}$ (m)	$v_{0.4}$ (m s^{-1})	V (m s^{-1})	$V/v_{0.4}$ (m s^{-1})	$v_{2\&8}$ (m s^{-1})	v_{486} (m s^{-1})
Blue River	66-12-14	0.732	C	0.358	0.47	0.406	0.864	0.425	0.404
Blue River	66-12-14	0.732	C	0.331	0.68	0.553	0.813	0.585	0.585
Blue River	67-03-20	0.610	C	0.431	0.73	0.582	0.800	0.600	0.628
Coal River	66-12-10	1.067	C	0.582	0.82	0.645	0.787	0.605	0.705
Cottonwood River	66-12-15	0.732	C	0.388	0.85	0.705	0.829	0.740	0.731
Cottonwood River	66-12-15	0.671	C	0.311	0.87	0.717	0.824	0.755	0.748
Dease River	66-12-17	2.225	C	0.309	0.41	0.357	0.870	0.365	0.410
Dease River	67-03-15	1.341	C	0.267	0.36	0.302	0.839	0.300	0.461
Dease River	67-03-15	1.615	C	0.417	0.34	0.279	0.821	0.290	0.292
Dezadeash River	67-04-14	1.097	C	0.348	1.37	0.992	0.724	0.940	1.178
Frances River	66-12-06	1.676	C	0.598	0.48	0.374	0.779	0.375	0.413
Hyland River	66-12-09	1.494	C	0.303	1.14	0.951	0.834	0.950	0.980
Hyland River	66-12-09	2.012	C	0.259	1.09	0.881	0.808	0.820	0.937
Iskut River	67-01-18	1.920	C	0.585	0.21	0.181	0.862	0.180	0.181
Iskut River	67-01-18	1.829	C	0.528	0.20	0.152	0.760	0.155	0.172
Iskut River	67-03-15	1.920	C	0.484	0.23	0.214	0.930	0.230	0.198
Iskut River	67-01-13	1.829	C	0.465	0.92	0.805	0.875	0.820	0.791
Kechika River	66-12-08	1.219	C	0.300	1.19	0.978	0.822	1.000	1.023
Kechika River	66-12-08	1.585	C	0.285	1.06	0.885	0.835	0.890	0.912
Kechika River	67-03-17	1.036	C	0.388	1.05	0.883	0.841	0.905	0.903
Liard River at lower crossing	66-12-12	3.475	C	0.459	1.16	0.994	0.857	1.005	0.998
Liard River at lower crossing	66-12-12	3.261	C	0.431	1.12	0.930	0.830	0.930	0.963
Liard River at upper crossing	66-12-07	4.511	C	0.547	1.21	1.008	0.833	1.035	1.041
Liard River at upper crossing	67-03-21	3.353	C	0.490	0.48	0.409	0.852	0.430	0.413
Lubbock River	67-01-16	2.042	C	0.093	0.59	0.472	0.800	0.445	0.507
M'Clintock River	67-02-03	1.189	C	0.340	0.33	0.280	0.848	0.295	0.284
Stewart River at crossing	66-11-17	1.890	C	0.362	0.31	0.277	0.894	0.280	0.267
Stewart River at crossing	66-11-17	2.103	C	0.274	0.27	0.244	0.900	0.250	0.232
Stewart River at crossing	67-01-26	1.981	C	0.261	0.42	0.304	0.274	0.320	0.361
Stewart River at Mayo	66-11-16	3.780	C	0.484	0.16	0.140	0.875	0.140	0.138
Stewart River at Mayo	66-11-16	7.071	C	0.441	0.26	0.217	0.835	0.225	0.224
Stewart River at Mayo	67-01-27	5.608	C	0.097	0.14	0.100	0.714	0.100	0.120
Stewart River at mouth	64-04-16	2.865	C	0.260	0.31	0.277	0.894	0.270	0.270
Pelly River at Ross River	66-11-23	1.829	C	0.537	0.68	0.548	0.806	0.550	0.585
Pelly River at Ross River	66-11-23	2.103	C	0.335	0.78	0.693	0.890	0.715	0.671
Pelly River at Ross River	67-01-31	1.524	C	0.336	0.37	0.339	0.916	0.350	0.318
Pelly River at Ross River	67-01-31	1.219	C	0.696	0.36	0.345	0.958	0.335	0.310
Pelly River at crossing	67-01-25	1.402	C	0.289	0.86	0.686	0.798	0.715	0.740
Stikine River at Telegraph Creek	67-01-22	2.530	C	0.229	0.50	0.427	0.854	0.440	0.430
Stikine River at Telegraph Creek	67-01-22	2.530	C	0.266	0.59	0.521	0.883	0.560	0.507
Stikine River at Telegraph Creek	67-03-20	1.829	C	0.290	0.62	0.543	0.876	0.550	0.533
Stikine River at Telegraph Creek	67-03-20	2.225	C	0.322	0.68	0.603	0.887	0.615	0.585
Stikine River below Klappan River	67-01-19	1.646	C	0.293	0.81	0.718	0.886	0.745	0.697
Swift River	66-12-18	1.859	C	0.559	0.91	0.805	0.885	0.825	0.783
Swift River	66-12-18	2.713	C	0.706	0.68	0.593	0.872	9.635	0.585
Swift River	66-02-10	1.554	C	0.331	0.63	0.513	0.814	0.500	0.542
Swift River	66-02-10	0.975	C	0.284	0.67	0.521	0.778	0.565	0.576
Swift River	67-03-22	1.859	C	0.455	0.55	0.493	0.896	0.515	0.473

*Ice conditions: C = clear; F = frazil; U = unknown.

Table 5. Continued

1	2	3	4	5	6	7	8	9	10
Location	Date	Depth (m)	Ice conditions*	$\frac{z_{max}}{D}$ (m)	$v_{0.4}$ ($m\,s^{-1}$)	V ($m\,s^{-1}$)	$V/v_{0.4}$ ($m\,s^{-1}$)	$v_{2\&8}$ ($m\,s^{-1}$)	v_{486} ($m\,s^{-1}$)
Teslin River	66-02-11	1.494	U	0.269	0.48	0.421	0.877	0.440	0.413
Teslin River	66-02-11	1.676	U	0.375	0.53	0.460	0.868	0.470	0.456
Teslin River	66-02-11	1.402	U	0.245	0.45	0.372	0.827	0.375	0.387
Watson River	66-11-30	0.640	C	0.239	0.37	0.321	0.868	0.320	0.318
Watson River	66-11-30	0.640	C	0.321	0.43	0.364	0.847	0.360	0.370
Watson River	67-04-05	0.457	C	0.265	0.39	0.322	0.826	0.340	0.335
Yukon River at Dawson	59-02-18	4.846	C	0.345	0.29	0.263	0.907	0.260	0.249
Yukon River at Dawson	60-02-16	4.328	U	0.618	0.56	0.501	0.895	0.500	0.482
Yukon River at Dawson	60-02-16	3.810	U	0.581	0.72	0.651	0.904	0.660	0.619
Yukon River at Dawson	60-02-16	3.261	U	0.511	0.78	0.694	0.890	0.715	0.671
Yukon River at Dawson	60-02-16	3.749	U	0.634	0.69	0.658	0.954	0.690	0.593
Yukon River at Dawson	63-04-09	6.858	U	0.470	0.52	0.468	0.900	0.520	0.447
Yukon River at Dawson	63-04-09	6.919	U	0.171	0.28	0.224	0.800	9.250	0.241
Yukon River at Hootalinqua	66-02-12	2.438	U	0.319	1.26	1.002	0.795	1.030	1.084
Yukon River at Hootalinqua	66-02-12	2.012	U	0.336	1.02	0.822	0.806	0.785	0.877
Yukon River at Hootalinqua	66-02-12	2.530	U	0.308	1.19	1.013	0.851	1.110	1.023
Yukon River at Whitehorse	67-02-15	3.597	C	0.317	0.48	0.420	0.875	0.425	0.413
Yukon River below White River	59-02-22	4.724	U	0.471	0.43	0.394	0.916	0.395	0.370
White River	67-04-25	2.377	U	0.536	0.66	0.572	0.867	9.575	0.568
Takhini River	66-12-27	1.219	C	0.436	0.74	0.649	0.877	0.650	0.636
Takhini River	66-11-14	3.018	C	0.528	0.61	0.553	0.907	0.535	0.525
Takhini River	66-11-15	2.377	C	0.573	0.60	0.514	0.857	0.550	0.516
Takhini River	66-11-15	2.591	C	0.531	0.47	0.390	0.830	0.425	0.404
Takhini River	66-11-16	2.377	C	0.547	0.67	0.542	0.810	0.560	0.576
Takhini River	66-11-16	2.530	C	0.605	0.52	0.455	0.875	0.505	0.447
Takhini River	66-11-17	2.530	C	0.557	0.64	0.569	0.889	0.585	0.550
Takhini River	66-11-18	2.530	C	0.532	0.70	0.609	0.870	0.640	0.602
Takhini River	66-11-18	2.377	C	0.643	0.45	0.448	0.996	0.485	0.387
Takhini River	66-11-19	2.804	C	0.500	0.70	0.603	0.861	0.630	0.602
Takhini River	66-11-22	1.920	C	0.575	0.48	0.397	0.827	0.450	0.413
Takhini River	67-02-08	1.372	C	0.486	0.47	0.434	0.923	0.450	0.404
Takhini River	56-03-27	0.610	C	0.323	0.57	0.482	0.846	0.500	0.490
Takhini River	65-12-28	1.097	C	0.275	0.66	0.571	0.865	0.550	0.568
Takhini River	65-12-28	1.219	C	0.329	0.70	0.568	0.811	0.575	0.602
Takhini River	65-12-28	1.280	C	0.441	0.71	0.590	0.831	0.615	0.611
Takhini River	65-12-28	0.518	C	0.359	0.45	0.380	0.844	0.380	0.387
Takhini River	65-12-28	0.914	C	0.262	0.59	0.497	0.842	0.500	0.507
Takhini River	67-02-09	0.914	C	0.262	0.78	0.687	0.881	0.695	0.671
Takhini River	67-02-02	0.823	C	0.358	0.60	0.557	0.928	0.580	0.516
Takhini River	67-02-07	0.975	C	0.295	0.57	0.480	0.842	0.480	0.490
Takhini River	67-01-28	0.884	C	0.216	0.60	0.530	0.883	0.550	0.516
Takhini River	67-01-28	0.823	C	0.235	0.59	0.503	0.853	0.510	0.507
Takhini River	67-01-04	1.097	C	0.351	0.75	0.657	0.876	0.600	0.645
Yukon River at Whitehorse (M)	83-12-14	2.62	F	0.464	1.02	0.877	0.859	0.840	0.877
Yukon River at Whitehorse (M)	83-12-14	4.51	F	0.530	1.01	0.894	0.885	0.970	0.869
Yukon River at Whitehorse (M)	83-12-14	3.47	F	0.436	1.19	1.054	0.885	1.075	1.023
Yukon River at Whitehorse (M)	84-01-06	3.05	F	0.337	1.39	1.142	0.822	1.155	1.195
Yukon River at Whitehorse (M)	84-01-06	3.9	F	0.282	1.36	1.207	0.888	1.240	1.170
Yukon River at Whitehorse (M)	84-01-06	3.96	F	0.461	1.16	0.978	0.843	0.980	0.998
Yukon River at Whitehorse (BM)	84-01-12	2.87	F	0.500	0.90	0.784	0.871	0.805	0.774
Yukon River at Whitehorse (AM)	84-01-23	4.45	F	0.295	0.88	0.762	0.866	0.765	0.757
Yukon River at Whitehorse (AM)	84-01-23	3.32	F	0.348	0.65	0.542	0.834	0.575	0.559
Yukon River at Whitehorse (AM)	84-01-23	3.2	F	0.252	0.97	0.786	0.810	0.795	0.834

Table 5. Continued

1	2	3	4	5	6	7	8	9	10
Location	Date	Depth (m)	Ice conditions*	$\frac{z_{max}}{D}$ (m)	$v_{0.4}$ (m s^{-1})	V (m s^{-1})	$V/v_{0.4}$ (m s^{-1})	$v_{2\&8}$ (m s^{-1})	v_{486} (m s^{-1})
Yukon River at Whitehorse (M)	84-02-07	2.74	F	0.225	1.23	1.129	0.918	1.170	1.058
Yukon River at Whitehorse (M)	84-02-07	3.51	F	0.333	1.29	1.193	0.925	1.195	1.109
Yukon River at Whitehorse (M)	84-03-01	3.08	F	0.360	1.24	1.062	0.856	1.050	1.066
Yukon River at Whitehorse (M)	84-03-01	3.35	F	0.316	1.27	1.077	0.848	1.090	1.092
Yukon River at Whitehorse (M)	84-03-01	2.04	F	0.448	1.05	0.799	0.760	0.855	0.903
Yukon River at Whitehorse (M)	84-03-08	2.87	F	0.448	1.00	0.853	0.853	0.870	0.860
Yukon River at Whitehorse (M)	84-03-14	3.66	F	0.521	1.01	0.898	0.889	0.925	0.869
Yukon River at Whitehorse (M)	84-03-14	3.29	F	0.494	0.97	0.816	0.841	0.810	0.834
Yukon River at Whitehorse (BM)	84-03-16	3.05	F	0.461	0.74	0.602	0.814	0.640	0.636
Yukon River at Whitehorse (BM)	85-12-12	3.719	F	0.284	1.25	1.129	0.903	1.135	1.075
Yukon River at Whitehorse (BM)	85-12-12	3.719	F	0.247	1.29	1.156	0.896	1.180	1.109
Yukon River at Whitehorse (BM)	85-12-20	3.658	F	0.276	1.22	1.111	0.911	1.200	1.049
Yukon River at Whitehorse (BM)	85-12-20	3.658	F	0.331	1.18	1.069	0.906	1.080	1.015
Yukon River at Whitehorse (BM)	86-01-06	3.444	F	0.332	1.09	1.041	0.955	1.100	0.937
Yukon River at Whitehorse (M)	85-12-23	3.078	F	0.404	1.27	1.111	0.875	1.105	1.092
Yukon River at Whitehorse (M)	85-12-23	3.078	F	0.393	1.26	1.105	0.877	1.145	1.084
Yukon River at Whitehorse (M)	85-12-23	3.078	F	0.376	1.34	1.150	0.858	1.165	1.152
Yukon River at Whitehorse (M)	86-01-14	2.957	F	0.473	1.17	1.099	0.939	1.115	1.006
Yukon River at Whitehorse (M)	85-02-15	3.600	C	0.313	1.52	1.306	0.859	1.390	1.307
Yukon River at Whitehorse (M)	85-02-15	3.600	C	0.394	1.59	1.341	0.843	1.395	1.367
Yukon River at Whitehorse (M)	85-02-15	3.600	C	0.373	1.51	1.313	0.870	1.330	1.299
Yukon River at Whitehorse (M)	85-02-15	3.600	C	0.409	1.56	1.322	0.847	1.310	1.342
Yukon River at Whitehorse (M)	85-02-15	1.716	F	0.543	0.83	0.696	0.839	0.675	0.719
Yukon River at Whitehorse (M)	85-02-15	1.716	F	0.537	0.87	0.735	0.844	0.735	0.748
Yukon River at Whitehorse (M)	85-02-15	1.716	F	0.543	0.91	0.778	0.855	0.770	0.783
Yukon River at Whitehorse (M)	85-02-15	1.716	F	0.541	0.88	0.783	0.890	0.790	0.757
Yukon River at The Thirty Mile	85-02-22	3.200	C	0.630	0.19	1.137	0.955	1.175	1.023
Mean				0.396			0.858		
Std. dev.				0.125			0.047		

As shown in Table 5, the average depth at which the velocity maximum occurs is 0.40 (std. dev. = 0.12) of total depth, and the coefficient R = 0.86 (std. dev. = 0.05), supporting our earlier observations (Alford and Carmack, 1987a).

Columns 9 and 10 in Table 5 also give a comparison of mean velocity estimates obtained by numerical integration to those obtained by the "conventional" and "486" methods. The "486" method compares well with the control estimate of V.

Using the "486" method, a number of streamflow measurements were made during the winter of 1985/86, and the results were compared to simultaneous streamflows recorded at the Whitehorse Rapids hydro site and to measurements using the traditional (0.2 and 0.8) method. These results (Table 6) suggest the "486" method is well worth considering for survey work; it is not only operationally faster, it is at least equivalent in accuracy to the traditional method.

DISCUSSION

Observations of the freezing sequence of the Yukon River from Lake Laberge to Whitehorse (see also Carmack *et al.*, 1987), suggest a pattern representative of many northern rivers that are oriented in a north south direction. The lower reach near Lake Laberge is dominated by the freezing in place of floes, due to the large amount of edge ice available upstream. Closer to the dam at Whitehorse, however, the supply of edge-derived floes is less, and the general pattern described in this report predominates.

Table 6. Verification of the "486" Method Using the Discharge at the Whitehorse Rapids Hydro Site as a Control

Date	Section	No. verticals per section	Streamflow ($m^3 s^{-1}$) At NCPC dam	"Conventional" method	"486" method	Percentage of difference to NCPC "Conventional"	"486"
85-11-18	Yukon at BM	13	152	154	153	1.3	0.6
85-11-25	Yukon at M	10	130	125	123	-3.8	-5.4
85-11-26	Yukon at BM	12	137	140	134	2.2	-2.2
85-12-02	Yukon at X1	11	130	125	–	-3.8	–
85-12-04	Yukon at BM	14	136	139	–	2.2	–
85-12-05	Yukon at X1	12	134	118	–	-11.9	–
85-12-06	Yukon at M	16	140	144	–	2.8	–
85-12-12	Yukon at BM	–	139	–	139	–	0
85-12-18	Yukon at M	16	141	144	141	2.1	0
85-12-20	Yukon at BM	–	–	–	–	–	–
85-12-23	Yukon at M	–	140	–	144	–	2.8
86-01-06	Yukon at BM	–	130	–	128	–	-1.5
86-01-08	Yukon at AM	20	134	137	137	2.2	2.2
86-01-10	Yukon at X1	16	131	124	128	-5.3	-2.3
86-01-14	Yukon at M	–	126	–	127	–	0.8
86-01-16	Yukon at BM	20	123	131	120	6.5	-2.4
86-02-04	Yukon at AM	20	117	125	119	6.8	1.7
86-02-05	Yukon at X1	23	118	–	115	–	-2.5
86-02-06	Big Salmon	25	–	21.0	21.4	–	–
86-02-10	Yukon at M	22	117	–	112	–	-4.3
86-02-12	Yukon at BM	22	117	–	115	–	-1.7
86-03-11	Yukon at M	24	110	–	110	–	-4.3
86-03-12	Yukon at BM	20	115	–	105	–	-8.6
86-03-21	Yukon at X1	26	100	–	110	–	0.9
86-03-24	Yukon at M	21	114	–	119	–	4.4
86-03-25	Yukon at BM	20	115	–	110	–	-4.0
86-04-04	Yukon at M	25	145	–	149	–	2.8
86-04-14	Yukon at BM	22	134	–	137	–	2.2

Table 7. Summary Comparison of the Winters of 1983/84, 1984/85, and 1985/86

Event	Winter 1983/84	1984/85	1985/86
Date of ice front at X4	–	–	Nov. 9
Date of ice front at BM	Dec. 4	Dec. 9	Nov. 11
Date of ice front at M	Dec. 9	Dec. 13	Nov. 17
Date of ice front at AM	Jan. 2	Dec. 29	Dec. 24
Date of ice front at X0	–	–	Jan. 28
Maximum ice thickness at M	1.0 m	0.7 m	1.0 m
Date of maximum ice thickness at M	Feb. 7	Mar. 19	Mar. 11
Maximum percentage area of frazil dam at M	41.6%	39.8 %	44%
Date of maximum percentage area of frazil dam at M	Dec. 14	Feb. 12	Nov. 25
Maximum water level at M	3.501 m	3.471 m	3.341m
Date of maximum water level at M	Dec. 9	Dec 16	Nov. 16
Maximum water level at AM	4.812 m	5.085 m	4.420 m
Date of maximum water level at AM	Jan. 1	Dec. 30	Dec. 4
Date of ice clear at depot	Mar. 22	Apr. 8	Apr. 17
Date of ice clear at AM	Mar. 23	Apr. 8	Apr. 18
Date of ice clear at M	Mar. 25	Apr. 10	Apr. 19
Date of ice clear at BM	Mar. 29	Apr. 12	Apr. 19
Snowfall from Nov. 1 to Mar. 31	0.724 m	1.672 m	127.6 m

Table 7 gives a summary comparison of the winters of 1983/84, 1984/85, and 1985/86. In general, the winter of 1985/86 was mild, but characterized by short duration extremes in both temperature and snowfall. In particular, at freeze-up air temperatures were below normal, while snowfall was two to three times above normal. Conversely, the midwinter period was characterized by higher than average temperatures and lower than normal snowfall. In the third year of study, the dates of freeze-up were nearly a month earlier than the previous year at BM and M, but only five days earlier at AM due to the period of warm weather that existed while the ice front moved from M to AM. Breakup was eight to ten days later due to the record low temperatures that occurred in early April.

Freeze-up jams and ice bridging can occur in the narrows at X4, at X0 near the depot, and immediately above the midchannel pier on the Robert Campbell Bridge. Ice bridging is a precursor of ice front formation and advance. In turn, the highest water levels occur during the time the ice front advances between M and AM; hence, this is a critical time for proper operation of the dam.

In general, ice front advance is most rapid above M, and relatively slow thereafter. Within this general pattern, however, the three years of study show that the rate of ice front advance can vary. This is partly due to differences in critical velocity at the front as conditioned by changes in surface slope; this velocity changes as frazil dams form and erode downstream. Hence, conditions determining whether a given floe will jam or submerge under the front are highly variable (see Michel, 1971).

Open leads may persist through winter at M and immediately below the bridge. While there were no extensive leads above the bridge that remained open during 1985/86, as in the previous winter, there were several areas of open water formed by jamming of irregular floes derived from the calving of edge ice during warm periods. For all three winters, and probably all winters, the water remained open from a point 350 m upstream from the bridge to the dam.

Breakup, while slightly increasing the hydraulic resistance of the reach, has little effect on water level.

Our observations on frazil dam structure lead us to believe that there are several types of frazil dams: some are influenced by stream geometry (i.e., bars, bends, narrows); some by velocity patterns (i.e., core velocity, eddies); and some by the roughness of the underside of the cover (i.e., projections, upended pans). Those predominantly influenced by stream geometry (e.g., the dam at Marwell) are likely to form at the same location each year and exhibit the same cross-sectional profile and area from year to year. Also, such dams appear to grow in size until the cover stabilizes (immediately after freeze-up) and then gradually erode to breakup. However, dams whose formation is precipitated by the highly irregular cover in the vicinity of an ice front, and thus in the path of the core velocity, appear to be subject to far more rapid erosion; the dam at X1 is an example.

There can be composite dams. Frazil may first accumulate under edge ice in the form of lateral deposition. Then, when the main channel is completely covered, midchannel or medial deposition may occur in the region where velocities are highest and the ice is roughest. In this case, the newly formed dam may cause the flow to bifurcate, thus affecting the conveyance capacity of the channel. Also, this deflection of the main flow may cause the older, lateral dam to erode.

Finally, we note that the "486" method, evaluated in this report, could significantly benefit those engaged in winter hydrometric surveys. The field time saved by taking a single measurement at each vertical station along a metering section could either result in considerable saving of time or, preferably, allow time for the placing of more closely spaced verticals. The former could be of importance in making better use of the available daylight hours for flying. The latter would allow better resolution of the horizontal current shear, better determination of the frazil dam cross-sectional area, and less chance of missing flow that may have been diverted into side channels. For example, it is not uncommon for frazil dams located upstream from the selected metering section to deflect the flow into channels that are anomalous with bed geometry.

ACKNOWLEDGMENTS

We would like to acknowledge the enthusiastic help of E. Marles and V. Chamberlain in the work of data collection and data reduction. Computer programming required for this analysis was done by R. Weigand, presently of SciTech Consultants Inc., Vancouver. Drafting and illustrating were ably done by B. Gordon of Gordon Enterprises, Vancouver.

We are also grateful to the staff at the Whitehorse Rapids hydro site for providing streamflow data, and to Arctic Diamond Drilling Ltd. in Marwell for allowing us daily passage through its property.

REFERENCES

Alford, M.E., and E.C. Carmack. 1987a. Observations on ice cover and streamflow in the Yukon River near Whitehorse during 1983/84. NHRI Pap. No. 32, Sci. Ser. No. 152, National hydrology Research Institute, Inland Waters/Lands Directorate, Environment Canada, Saskatoon, Sask.

Alford, M.E., and E.C. Carmack. 1987b. Observations on ice cover and streamflow in the Yukon River near Whitehorse during 1984/85. NHRI Pap. No. 34, Sci. Ser. No. 155, National Hydrology Research Institute, Inland Waters/Lands Directorate, Environment Canada, Saskatoon, Sask.

Ashton, G.D., and J.F. Kennedy. 1972. Ripples on the underside of river ice covers. J. Hydraul. Eng., 98: 1603-24.

Carey, K.L. 1966. Observed configuration and computed roughness of the underside of river ice, St. Croix River, Wisconsin. U.S. Geol. Surv. Prof. Pap., 550-B: 192-98.

Carmack, E.C., R.C. Wiegand, E.M. Marles, M.E. Alford, and V.A. Chamberlain. 1987. Physical limnology of an ice-covered lake with through-flow: Lake Laberge, Yukon Territory. NHRI Pap. No. 35, Sci. Ser. No. 157, National Hydrology Research Institute, Inland Waters/Lands Directorate, Environment Canada, Saskatoon, Sask.

Gilpin, R.R., T. Hirrata, and K.C. Cheng. 1980. Wave formation and heat transfer at an ice-water interface in the presence of a turbulent flow. J. Fluid Mech., 99: 619-40.

Lau, Y.L. 1982. Velocity distributions under floating covers. Can. J. Civ. Eng., 9: 76-83.

Martin, S. 1981. Frazil ice in rivers and oceans. Annu. Rev. Fluid Mech., 13: 379-97.

Michel, B. 1971. Winter regime of rivers and lakes. U.S. Army Corps Eng. Cold Reg. Res. Eng. Lab., Monograph 111-Bla, Hanover, N.H.

Osterkamp, T.E. 1978. Frazil ice formation: a review. J. Hydraul. Eng., 104: 1239-55.

Osterkamp, T.E., and J.P. Gosink. 1983. Frazil ice formation and ice cover development in interior Alaska streams. Cold Reg. Sci. Technol., 8: 43-56.

Papadakis, J.E., E.C. Carmack, and M.E. Alford. 1987. Velocity profiles under ice cover. In preparation.

Tsang, G. 1982. Frazil and Anchor Ice. National Research Council Subcommittee on Hydraulics of Ice Covered Rivers, Ottawa, Ont.